SYNTHESIS AND CHARACTERIZATION OF HYDROGENPHOSPHATE-STABILIZED NICKEL(0) NANOCLUSTERS AS CATALYST FOR THE HYDROLYSIS OF SODIUM BOROHYDRIDE

A THESIS SUBMITTED TO
THE GRADUATE SCHOOL OF NATURAL AND APPLIED SCIENCES
OF
MIDDLE EAST TECHNICAL UNIVERSITY

BY

ÖNDER METİN

IN PARTIAL FULFILLMENT OF THE REQUIREMENTS
FOR
THE DEGREE OF MASTER OF SCIENCE
IN
CHEMISTRY

MAY 2006

Approval of the Graduate School of Natural and Applied Sciences

_____

Prof.Dr. Canan Özgen
Director

I certify that this thesis satisfies all the requirements as a thesis for the degree of Master of Science.

_____

Prof. Dr. Hüseyin İşçi
Head of the department

This is to certify that we have read this thesis and that in our opinion it is fully adequate, in scope and quality, as a thesis for the degree of Master of Science.

_____

Prof. Dr. Saim Özkâr
Supervisor

Examining Committee Members

Prof. Dr. Hüseyin İşçi	(METU, CHEM)	_____
Prof. Dr. Saim Özkâr	(METU, CHEM)	_____
Prof. Dr. Işık Önal	(METU, CHE)	_____
Assoc.Prof. Dr. Gülsün Gökağaç	(METU, CHEM)	_____
Assist.Prof.Dr. Michael Pitcher	(METU, CHEM)	_____

I hereby declare that all information in this document has been obtained and presented in accordance with academic rules and ethical conduct. I also declare that, as required by these rules and conduct, I have fully cited and referenced all material and results that are not original to this work.

Name, Last name :

Signature :

ABSTRACT

SYNTHESIS AND CHARACTERIZATION OF HYDROGENPHOSPHATE-STABILIZED NICKEL(0) NANOCLUSTERS AS CATALYST FOR THE HYDROLYSIS OF SODIUM BOROHYDRIDE

Metin, Önder
M.S., Department of Chemistry
Supervisor: Prof. Dr. Saim Özkâr

May 2006, 62 pages

The development of new storage materials will facilitate the use of hydrogen as a major energy carrier in near future. In hydrogen economy, chemical hydrides such as $NaBH_4$, KBH_4, LiH, NaH have been tested as hydrogen storage materials for supplying hydrogen at ambient temperature. Among these chemical hydrides, sodium borohydride seems to be an ideal hydrogen storage material because it is stable under ordinary conditions and liberates hydrogen gas in a safe and controllable way in aqueous solutions. However, self hydrolysis of sodium borohydride is so slow that it requires a suitable catalyst. All of the prior catalysts tested for the hydrolysis of sodium borohydride are heterogeneous and, therefore, have limited activity because of the small surface area. Here, we report for the first time the employment of water dispersible metal(0) nanoclusters having a large portion of atoms on the surface as a catalyst for the hydrolysis of sodium borohydride.

In-situ formation of nickel(0) nanoclusters and catalytic hydrolysis of sodium borohydride were performed in the same medium. Nickel(0) nanoclusters are prepared from the reduction of nickel(II) acetylacetonate by sodium borohydride in aqueous solution and stabilized with hydrogenphosphate anions. The nickel(0) nanoclusters were characterized by using XPS, Powder XRD, FT-IR, UV-Vis and NMR spectroscopic methods. The kinetics of the nickel(0) nanoclusters catalyzed hydrolysis of sodium borohydride was studied depending on the catalyst concentration, substrate concentration, stabilizing agent concentration and temperature. Tha kinetic study shows that the nickel(0) nanocluster-catalyzed hydrolysis of sodium borohydride is first order with respect to catalyst concentration and zero order with respect to substrate concentration The activation parameters of this reaction were also determined from the evaluation of the kinetic data. The hydrogenphosphate-stabilized nickel(0) nanoclusters provide a lower activation energy (Ea= 55 kJ/mol) than bulk nickel (Ea=73 kJ/mol) for the hydrolysis of sodium borohydride.

Keywords: Nickel(0) nanoclusters, hydrolysis of sodium borohydride, heterogeneous catalyst, hydrogenphosphate, X-ray photoelectron spectroscopy (XPS), FT-IR, UV-Vis

ÖZ

SODYUM BORHİDRÜRÜN HİDROLİZİNİ KATALİZLEYEN HİDROJENFOSFAT İLE KARARLI HALE GETİRİLMİŞ NİKEL(0) NANOKÜMELERİNİN SENTEZLENMESİ VE TANIMLANMASI

Metin, Önder
Yüksek Lisans, Kimya Bölümü
Tez Yöneticisi: Prof. Dr. Saim Özkâr

Mayıs 2006, 62 sayfa

Yakın gelecekte, depolama tekniklerinin gelişimi ile hidrojenin enerji taşıyıcı olarak kullanılması büyük ölçüde kolaylaşacaktır. Hidrojen ekonomisinde, istenilen sıcaklıkta hidrojen eldesi için $NaBH_4$, KBH_4, LiH, NaH gibi kimyasal hidrürler hidrojen depolama malzemesi olarak test edilmektedir. Bu kimyasal hidrürler arasında, normal koşullarda kararlı, sulu çözeltisinde güvenli ve kontrollü bir şekilde hidrojen gazı elde edilen sodyum borhidrür, en ideal hidrojen depolama malzemesi olarak görünmektedir. Ancak, sodyum borhidrürün sulu çözeltisindeki hidrolizi çok yavaş olduğu için uygun bir katalizör kullanılması gerekmektedir. Sodyum borhidrürün hidrolizinde bugüne kadar kullanılan katalizörlerin hepsi heterojen katalizördür ve dolayısıyla yüzey alanlarının küçük olması nedeniyle düşük katalitik etkinliğe sahiptir. Bu nedenle, geniş yüzey alanına sahip metal(0) nanokümelerinin

katalizör olarak kullanılması, katalitik etkinliğin arttırılması için önemli bir yöntemdir.

Nikel(0) nanokümelerinin eş zamanlı oluşumu ve sodyum borhidrürün katalitik hidrolizi aynı ortamda gerçekleştirildi. Nikel(0) nanokümeleri, nikel(II) asetilasetonatın sulu çözeltide sodyum borhidrür ile indirgenmesi ile hazırlandı ve hidrojenfosfat anyonu ile kararlı hale getirildi. Sentezlenen nikel(0) nanokümeleri XPS (X-Ray Fotoelektron Spektroskopisi), Toz XRD, FT-IR, UV-Vis ve NMR spektroskopik yöntemleri ile tanımlandı. Nikel(0) nanokümeleri ile katalizlenen sodyum borhidrürün hidrolizi tepkimesinin kinetiği, katalizör derişimine, substrat derişimine, kararlaştırıcı iyon derişimine ve sıcaklığa bağlı olarak incelendi. Kinetik çalışmalar sonucunda nikel(0) nanokümeleri ile katalizlenen sodyum borhidrürün hidrolizi tepkimesinin katalizör derişimine göre birinci dereceden ve substrat derişimine göre sıfırıncı dereceden olduğu bulunmuştur. Kinetik verilerin değerlendirilmesi ile nikel(0) nanokümeleri ile katalizlenen sodyum borhidrürün hidrolizi tepkimesinin aktivasyon parametreleri belirlenmiştir ve hidrojenfosfat ile kararlı hale getirilmiş nikel(0) nanokümelerinin sodyum borhidrürün hidrolizi tepkimesi için külçe nikele göre daha düşük aktivasyon enerjisi sağladığı bulunmuştur.

Anahtar kelimeler: Nikel(0) nanokümeleri; Sodyum borhidrürün hidrolizi; Hidrojenfosfat, Heterojen katalizör, X-ışınları fotoelektron spektroskopisi (XPS); FT-IR, UV-Görünür Spektroskopisi.

To My Family

ACKNOWLEDGEMENTS

I would like to express my sincere gratitude to Prof. Dr. Saim Özkâr for his great support, supervision and understanding throughout in this study.

I would like to thank Mehmet Zahmakıran, Murat Rakap, Ercan Bayram, F.Sanem Koçak, Dilek Ayşe Boğa, and Ezgi Keçeli for their caring, never ending helps and their encouragement during my study.

I also express my thanks to Chemistry Department of Middle East Technical University for providing facilities used in this study.

The last but not least, I would like to extend my gratitude to my father, Ramazan, my mother, Rabiye for helping me with every problem I encountered during the whole study.

TABLE OF CONTENTS

LIST OF TABLES

TABLE

LIST OF FIGURES

CHAPTER 1

INTRODUCTION

Fossil fuels (i.e., petroleum, natural gas, and coal) will overwhelmingly be used to meet the increasing worldwide energy demand at least for the next few decades [1]. There has been a growing interest in the use of renewable energy sources such as solar and wind energy because of increasing concern about the environmental problems, including global warming caused by the emission of gases from the combustion of fossil fuels. However, besides their relatively high cost, energy production from renewable sources has the problem of discontinuity, for example, solar energy is not always available. The obvious solution to this predicament is the energy storage. In this context, hydrogen appears to be the best energy carrier as it has an abundant and secure source, clean, renewable, and widely available from diverse sources [2]. Dramatic improvements, particularly in the existing technologies for production, storage, and usage of hydrogen, are still needed if hydrogen is to become a major energy carrier in the future. The hydrogen-based energy economy deals with the development of diversity of sources for hydrogen production using efficient technologies, finding viable methods for hydrogen storage, lowering the cost of fuel cells and improving their on-board usage. Chemical hydrides seem to be ideal for hydrogen storage in the solid-state. Among the chemical hydrides sodium borohydride, $NaBH_4$, has been suggested as a new fuel source for supplying hydrogen under mild conditions [3]. The hydrolysis of sodium borohydride produces hydrogen gas and water-soluble sodium metaborate, $NaBO_2$, in the presence of a suitable catalyst. By this way, hydrogen can be generated safely for fuel cells.

$$NaBH_4 + 2H_2O \xrightarrow{\text{catalyst}} NaBO_2 + 4H_2 \qquad \textbf{(1)}$$

Generating H_2 catalytically from $NaBH_4$ solutions has many advantages: $NaBH_4$ solutions are nonflammable, the reaction products are environmentally benign, the rate of H_2 generation can be easily controlled, the reaction product $NaBO_2$ can be recycled, H_2 can be generated even at low temperatures. This reaction can be accelerated by catalyst, by acid, or under elevated temperature. The hydrolysis occurs to some extent even without a catalyst if the solution has $pH < 9$. The key feature of catalyzed reaction to produce H_2 is that H_2 generation in alkaline ($pH > 9$) $NaBH_4$ solutions, occurs only when these solutions are in contact with selected heterogeneous catalysts. Without catalyst present, strongly basic $NaBH_4$ solutions do not produce appreciable H_2. This reaction is extremely efficient on a weight basis, since out of 4 moles of H_2 that is produced, half comes from $NaBH_4$, and the other half from H_2O. Also the reaction is exothermic, so no energy input is needed to generate H_2.

A variety of transition metal compounds have been reported as catalyst for this hydrolysis reaction [4,5,6,7,8,9,10,11]. However, all of the prior catalysts tested for the hydrolysis of sodium borohydride are heterogeneous and, therefore, have limited activity because of the small surface area. A recent paper has reported for the first time the employment of water dispersible ruthenium(0) nanoclusters having large portion of atoms on the surface as catalyst for the hydrolysis of sodium borohydride [12], using the knowledge that metal nanoclusters with large surface area can provide high catalytic activity [13]. It has been showed that water dispersible ruthenium(0) nanoclusters have the highest catalytic activity for the hydrolysis of sodium borohydride even at ambient temperatures; also much more active than the bulk ruthenium metal [8,14]. Nickel, which is widely used catalyst for the hydrogenation of olefins, has also been employed as catalyst for the hydrolysis of sodium borohydride [4]. However, it has been found to be less active than, for example, bulk ruthenium in the hydrolysis of sodium borohydride. Similar to the case of ruthenium [12], using nickel(0) nanoclusters is expected to increase the catalytic activity.

This anticipation stimulated us to investigate the water dispersible nickel(0) nanoclusters as catalyst in the hydrolysis of sodium borohydride. A literature search resulted in no report on the water-dispersible nickel(0) nanoclusters. Here, we report for the first time the synthesis and use of water-dispersible hydrogenphosphate-stabilized nickel(0) nanoclusters as catalyst in the hydrolysis of sodium borohydride. HPO_4^{2-} ion has been predicted to be a suitable anionic stabilizer for the nickel(0) nanoclusters by lattice size-matching model, as it has O–O distance perfectly matching to the metal-metal distance of ca. 2.50Å in the nickel(0) nanoclusters [15]. Although previously unappreciated, as tridentate binding, chelating oxygen-donor ligand with -2 charge, hydrogenphosphate has recently been shown to be excellent stabilizer for the iridium(0) nanoclusters [16]. Additionally, HPO_4^{2-} is an inorganic anion soluble in water and, therefore, it was chosen as stabilizer in the preparation of water-dispersible nickel(0) nanoclusters that will be used as catalyst in the hydrolysis of sodium borohydride. The catalytic activity and stability of nickel(0) nanoclusters were studied depending on the stabilizer concentration, and the optimum concentration of hydrogenphosphate ion was found. The kinetics of the hydrolysis of the sodium borohydride catalyzed by the nickel(0) nanoclusters was studied depending on the catalyst concentration, substrate concentration and the temperature. The reaction order, activation energy and activation parameters of catalytic hydrolysis reaction were found in the light of kinetic study of the hydrogenphosphate-stabilized nickel(0) nanoclusters catalyzed hydrolysis of sodium borohydride.

In addition to investigation of catalytic hydrolysis of sodium borohydride, our work also provides a fundamental understanding of the formation and stabilization of transition metal nanoclusters in aqueous media. This understanding is important in the preparation of transition metal nanoclusters which are stable as a dispersed phase, but still catalytically active for example, in the hydrolysis of sodium borohydride.

CHAPTER 2

HYDROGEN ECONOMY

2.1. Global energy Problems

Energy, as one of the most important input of the economic and social development, has been one of the key sectors in the global economy. In the last decade, major changes took place in this part of the world leading to new strategies especially in the energy globalization process with an increasing trend. One of the most weighted components of economic and social development of the nations is their efforts towards materializing energy based projects [17].

World primary energy demand is expected to increase more than 60% between 2000 and 2030 [1]. By the end of 2002, world's primary energy production consisted of approximately 4.7 billion tons of coal, 3.5 billion tons of oil, and 2.6 trillion meter cubes of natural gas. These three fossil resources provide about 80% of the world's primary energy consumption and, 99% of the trade, as well. Furthermore, the growing number of people without access to very basic energy supplies indicated a rapid growth in demand in the coming years. The challenge lies on finding a way to harmonize the necessity and demand for energy supply with its impact on the natural resource base in order to ensure a sustainable path of development.

Hydrogen based energy technologies are today a major topic of international importance for energy supply and environmental protection. A number of countries and the European Union have announced certain programs on hydrogen based energy technologies. This strong interest at government level is echoed in the private sector where, investments in hydrogen technology have grown considerably over recent years leading to technology development for stationery and mobile fuel cells and hydrogen-fuelling facilities for fuel cell powered vehicles.

In the long term a hydrogen-based economy will have impact on all these sectors. In view of technological developments, vehicle and component manufacturers, transport providers, the energy industry, and even householders are seriously looking at alternative energy sources and more efficient and cleaner technologies-especially hydrogen and hydrogen-powered fuel cells [18].

2.2. Hydrogen as an Energy Carrier

Hydrogen is the simplest element; an atom consists of only one proton and one electron. It is also the most abundant element in the universe. Despite its simplicity and abundance, hydrogen does not occur naturally as a gas on the Earth, it is always combined with other elements. Hydrogen is also found in many organic compounds, notably the "hydrocarbons" that make up many of our fuels, such as gasoline, natural gas, methanol, and propane.

Hydrogen can be made by separating it from hydrocarbons by applying heat, a process known as "reforming" hydrogen [2]. Currently, most hydrogen is made this way from natural gas. An electrical current can also be used to separate water into its components of oxygen and hydrogen. Some algae and bacteria, using sunlight as their energy source, even give off hydrogen under certain conditions.

Hydrogen can form metal hydrides with some metals and alloys. During the formation of the metal hydride, hydrogen molecules are split and hydrogen atoms are inserted in spaces inside the lattice of suitable metals or alloys. In such a way an effective storage comparable to the density of liquid hydrogen is created. However, when the mass of the metal or alloy is taken into account then the metal hydride gravimetric storage density is comparable to the storage of pressurized hydrogen. The best achievable gravimetric storage density is about 10.7% by weight for metal hydride [19].

Hydrogen is high in energy, yet an engine that burns pure hydrogen produces almost no pollution. Fuel cells are a promising technology for use as a source of heat and electricity for buildings, and as an electrical power source for electric vehicles [20]. Although these applications would ideally run off pure hydrogen, in the near term they are likely to be fueled with natural gas, methanol, or even gasoline. Reforming these fuels to create hydrogen will allow the use of much of our current energy infrastructure gas stations, natural gas pipelines, etc. while fuel cells are phased in.

In the future, hydrogen could also join electricity as an important *energy carrier*. An energy carrier stores, moves, and delivers energy in a usable form to consumers. Renewable energy sources, like the sun, cannot produce energy all the time. The sun does not always shine. However, hydrogen can store this energy until it is needed and can be transported to where it is needed.

Hydrogen production, storage and distribution methods are commercially available today, but dramatic improvements, particularly of existing technologies, are needed if hydrogen is to become a major energy carrier in the future. As a result of the above discussion, the importance of hydrogen economy is getting increasing. The hydrogen based energy economy needs three basic research stages;

First, despite its abundance in nature, hydrogen is not a primary energy source and must be produced from a primary energy source such as fossil hydrocarbons or coal, nuclear fusion or fission, hydroelectric, or renewable energy sources. Depending on the source, its production may or may not involve CO_2 emissions.

Second, research is required for lowering the cost of fuel cells and improving their usage on-board systems. Hydrogen is an ideal anodic fuel for Proton Exchange Membrane, PEM, fuel cells that converts chemical energy of hydrogen into electrical energy. Until large PEM fuel cells become commercially available, internal combustion engines fueled with H_2 could represent a backup option for upcoming zero emission vehicle, ZEV. In internal combustion applications, H_2 can be considered more thermally efficient than gasoline primarily because it burns better in excess air, and permits use of higher compression ratios. H_2 can burn in lean as well as rich air mixtures; it can improve fuel use efficiencies in start-stop type of city driving.

Third research is needed advanced hydrogen storage concepts include metal hydrides, complex hydrides, carbon adsorption and nanostructured materials, carbon nano-tube encapsulation. A key criteria for successfully usage of hydrogen in the transportation market is the energy density of the storage system, as compared to other fuels.

Some experts think that hydrogen will form the basic energy infrastructure that will power future societies, replacing today's natural gas, oil, coal, and electricity infrastructures.

2.3. Sodium Borohydride as a Hydrogen Storage Material

The development of new storage materials will facilitate the use of hydrogen as a major energy carrier in the near future [2]. In hydrogen economy, chemical hydrides have been tested as hydrogen storage materials for supplying hydrogen under mild conditions. Among these chemical hydrides, sodium borohydride, $NaBH_4$, appears to be a promising hydrogen storage material as it provides a safe and practical mean of producing hydrogen and has a hydrogen content of 10.7 % by weight [21] shown in figure 2.1.

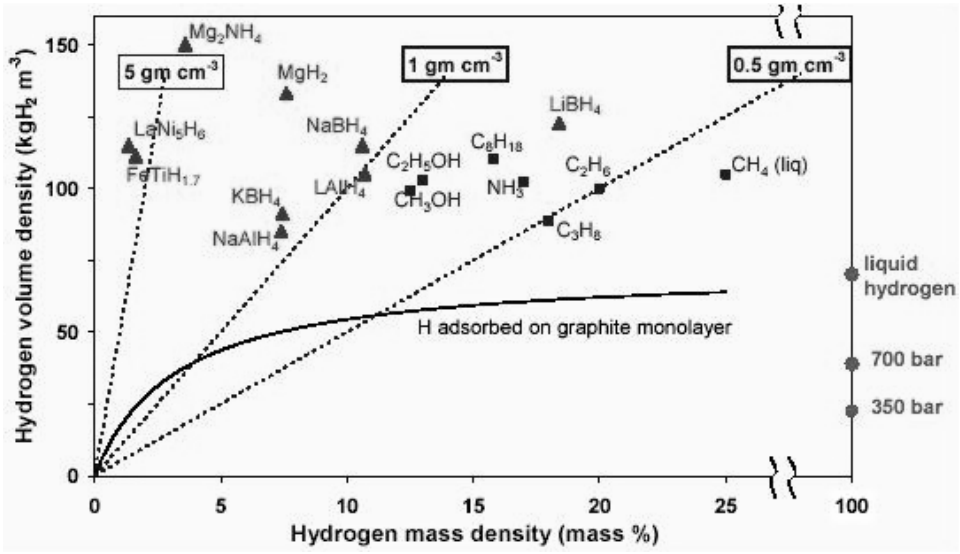

Figure 2.1. Volumetric hydrogen density versus gravimetric hydrogen density of various hydrogen containing compounds (taken from the literature[3]).

Sodium borohydride is stable in alkaline solution; however, hydrolysis in the presence of a suitable catalyst generates hydrogen gas in the amount twice its hydrogen content and also water-soluble sodium metaborate, $NaBO_2$, at moderate temperature [22]. By this way hydrogen can be generated safely for the fuel cells.

$$NaBH_4 + 2H_2O \xrightarrow{\text{catalyst}} NaBO_2 + 4H_2 \qquad \textbf{(1)}$$

Catalytic hydrogen gas generation from $NaBH_4$ solutions has many advantages: $NaBH_4$ solutions are nonflammable, the reaction products are environmentally benign, rate of H_2 generation is easily controlled, the reaction product $NaBO_2$ can be recycled, H_2 can be generated even at low temperatures. Such a hydrolysis of sodium borohydride can be accelerated by catalysts [23], by acid [24], or under elevated temperature [25].

This reaction occurs to some extent even without a catalyst if the solution pH < 9. However to increase the shelf life of $NaBH_4$ solutions (and to prevent H_2 gas from being slowly produced upon standing), $NaBH_4$ solutions are typically maintained as a strongly alkaline solution by adding NaOH. The key feature of using a catalyzed reaction to produce H_2 is that H_2 generation in alkaline (pH > 14) $NaBH_4$ solutions occurs only when these solutions contact selected heterogeneous catalysts. Without a catalyst, strongly alkaline $NaBH_4$ solutions do not produce appreciable H_2. This reaction is extremely efficient on a weight basis, since out of the 4 moles of H_2 that is produced, half comes from $NaBH_4$, and the other half from H_2O. The reaction is exothermic, so no energy input is needed to generate H_2.

The only other product of reaction, sodium metaborate (in solutions with pH > 11 the predominant solution product is sodium tetrahydoxyborate $NaB(OH)_4$), is water soluble and environmentally innocuous. Since the hydrolysis of sodium borohydride is completely inorganic reaction and does not contain sulfur, it produces virtually no fuel poisons such as sulfur compounds, carbon monoxide, soot, or aromatics. Therefore this reaction is considerably safer, more efficient, and more easily controllable than producing H_2 by other chemical methods [3]. The heat generated by the reaction 75 kJ/mole H_2 formed is considerably less than typical > 125 kJ/mole H_2, produced by reacting other chemical hydrides with water [26]. This promises a safer and more controllable reaction.

The catalysts tested for the hydrolysis of sodium borohydride, are chronologically, listed platinum or rhodium salts [22], cobalt salt [23], iron, ruthenium, palladium, osmium, iridium, and platinum salts [6], nickel, Raney nickel, and bulk cobalt [4], alloys such as $LaNi_{4.5}T_{0.5}$ (T = Mn, Cr, Co, Fe, Cu) [7], bulk ruthenium [8], mixed metal/metal oxides such as Pt-$LiCoO_2$ [9], nickel boride [10], and filamentary nickel-cobalt [11]. With the exception of metal salts of platinum, ruthenium and cobalt, all the catalyst used for the hydrolysis of sodium borohydride are heterogeneous. The limited surface area of heterogeneous catalysts restricts their catalytic activity to a low value. As the activity of a catalyst is directly related to its surface area, using water dispersible nanoclusters is a promising way to increase the catalytic activity.

CHAPTER 3

TRANSITION METAL NANOCLUSTERS

3.1. Colloidal Metal Nanoclusters

Nanoclusters are mono dispersed particles that are generally less than 10 nm (100 Å) in diameter [27] have generated intense interest over the past decade. One reason for this is the belief that nanoclusters will have unique properties, derived in part from the fact that these particles and their properties lie somewhere between those of bulk and single-particle species [28,29]. Nanoparticles have many fascinating potential uses, including quantum dots [30], quantum computers [31], quantum devices [32], chemical sensors [33], light-emitting diodes [34], ferrofluids for cell separations [35], and photochemical pattern applications such as flat-panel displays [36]. Nanoparticles also have significant potential as new types of highly active and selective catalysts [37].

Two reasons chemists believe that nanoclusters hold the potential to be more active and selective catalysts than those of today are that a large percentage of a nanoclusters' metal atoms lie on the surface, and that surface atoms do not necessarily order themselves in the same way that those in the bulk do [38]. Furthermore, the electrons in nanoclusters are confined to spaces that can be as small as a few atom-widths across, giving rise to quantum size effects [38]. Perhaps most importantly, nanoclusters offer the possibility of controlling both the nanocluster size and the surface ligands in a quantitative, modifiable and better understood way than previously possible for, say, supported heterogeneous catalysts.

When a metal particle with bulk properties is reduced to the nanometer size scale, the density of states in the valence and the conduction band decreases to such an extent that the quasi-continuous density of states is replaced by a discrete energy level structure and the electronic properties change dramatically. Figure 3.1 illustrates how more and more atoms are located on the surface of particles when a cube of metal divided into smaller and smaller cubes,

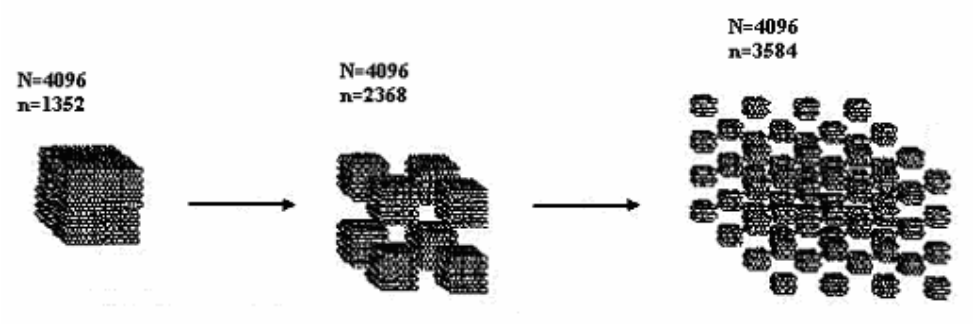

Figure 3.1. The effect of particle size on the ratio of the number of surface atoms to the total number of atoms. N= the total number atoms; n= the number of surface atoms.

To investigate the physical and chemical properties of transition metal nanoparticles, the preparation of these metal particles in monodispersed form and therefore a great degree of control over size, structure, and surface composition is essentially required.

3.2. Stabilization of Colloidal Metal Nanoparticles in Liquids

3.2.1. Electrostatic Stabilization

Before beginning a description of synthetic methods, a general and critical aspect of colloid chemistry should be considered, and that is the means by which the metal particles are stabilized in the dispersing medium, since small metal particles are unstable with respect to agglomeration to the bulk.

At short interparticle distances, two particles would be attracted to each other by Van der Waals forces and in the absence of repulsive forces two counteract this attraction an unprotected sol would coagulate. This counteraction can be achieved by two methods, electrostatic stabilization and steric stabilization [39]. In classic gold sol, for example, prepared by reduction of aqueous $[AuCl_4]^-$ by sodium citrate [40], the colloidal gold particles are surrounded by an electrical double layer formed by adsorbed citrate and chloride ions and cations which are attracted to them. This results in a coulombic repulsion between particles, and the net result is shown schematically in Figure 3.2.

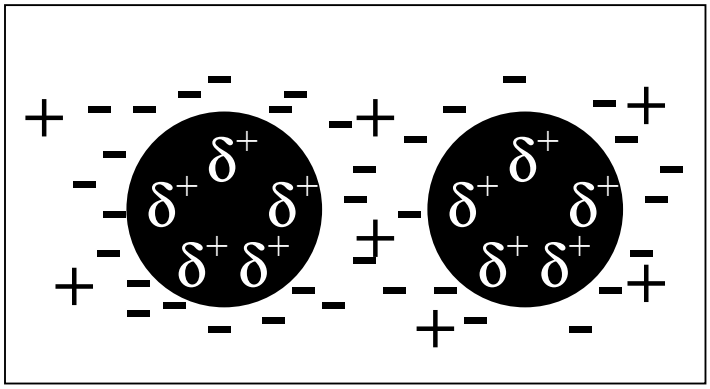

Figure 3.2. Schematic representation of electrostatic stabilization of metal colloid particles

The coulombic repulsion between the particles decays approximately exponentially with the particle distance. The weak minimum in potential energy defines a stable situation. Thus, if the electric potential resulting from the double layers is high enough, electrostatic repulsion prevents aggregation [41]. If the surface charge is reduced by the displacement of adsorbed anions by a more strongly binding neutral adsorbate, the colloidal particles can now collide and agglomerate under the influence of the Van der Waals attractive forces [42].

3.2.2. Steric Stabilization

Colloidal particles can be prevented from aggregating by the adsorption of molecules such as polymers, surfactants or ligands at the surface of the particles, thus providing a protective layer Figure 3.3. Polymers are widely used, and it is obvious that the protectant, in order to function effectively, must not only coordinate to the particle surface, but must also be adequately solvated by the dispersing fluid-such polymers are termed amphiphilic. The choice of polymer is determined by consideration of the solubility of the metal colloid precursor, the solvent of choice, and the ability of the polymer to stabilize the reduced metal particles in the colloidal state [28].

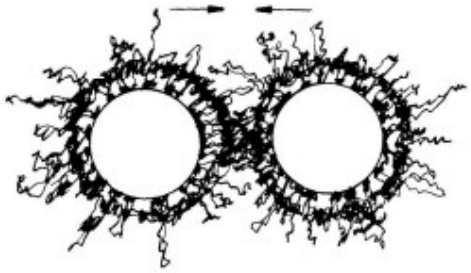

Figure 3.3. Schematic representation of steric stabilization of metal nanoparticles

3.2.3. Electrosteric Stabilization

Electrostatic and steric stabilization are in a sense combined in the use of long chain alkylammonium cations and surfactants, either in single-phase sols or in reverse micelle synthesis of colloidal metals. These compounds bear a polar head group able to generate an electrical double layer and a lyophilic side chain able to provide steric repulsion. The electrosteric stabilization can be also obtained from polyoxoanions such as the couple ammonium (Bu_4N^+)/polyoxoanion ($P_2W_{15}Nb_3O_{62}^{9-}$).

3.2.4. Stabilization By a Ligand or Solvent

The term ligand stabilization describes the use of traditional ligands to stabilize transition metal colloids. This stabilization occurs by the coordination of metallic nanoparticles with ligands such as phosphines, thiols, amines or carbon monoxide. For example, Au, Pt, Pd, and Ni colloids are stabilized by phosphines [43,44]**.** It has also been reported that nanoparticles can be stabilized only by solvent molecules [45].

3.3. Methods for the Preparation of Transition Metal Nanoparticles

The synthetic methods which have been used for the preparation of transition metal nanoclusters include modern versions of established methods of metal colloid preparation such as the mild chemical reduction of solutions of transition metal salts and complexes and newer methods such as radiolytic and photochemical reduction, metal atom extrusion from labile organometallics, and the use of metal vapor synthesis techniques. Some of these reactions have been in use for many years, and some are the results of research simulated by current resurgence in metal colloid chemistry. The list of preparation methods are being extended daily, and, some examples of this method are described below [28].

3.3.1. Chemical Reduction of Metal Salts

The reduction of transition metal salts in solution is the most widely practiced method of generating colloidal suspensions of metal. In aqueous systems, the reducing agent must be added or generated in situ, but in non-aqueous systems the solvent and reducing agent can be one and the same [28].

A wide range of reducing agents have been used to obtain colloidal materials, gas such as hydrogen or carbon monoxide, hydrides or salts such as sodium borohydride or sodium citrate, or even oxidizable solvents such as alcohols [46].

3.3.1.1. Alcohols

Some transition metal salts can be reduced in refluxing alcohol. In this process, the alcohol acts both as solvent and reducing agent. Generally, the alcohols, which are useful reducing agents, contain α-hydrogen. Thus, methanol, ethanol, or 2-propanol is good reducing agents, whereas *tert*-butyl alcohol is not effective. During the reduction, the alcohols are oxidized to the corresponding carbonyl compounds (Scheme 1). This reaction often requires the presence of water to be effective [46].

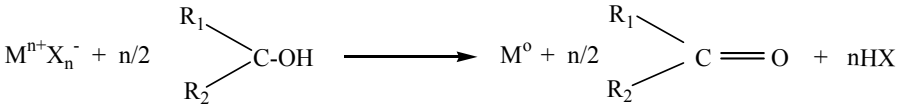

Scheme 1. Formation of Metallic Nanoparticles in Alcoholic Media

Rh, Pt, Pd, Os, or Ir colloidal transition metals are synthesized by using aqueous alcohols as reducing agent [47,48,49,50,51].

3.3.1.2. Hydrogen and Carbon Monoxide

Hydrogen is one of the most widely used reducing agents to prepare transition metal nanoparticles. Aqueous colloidal solutions of Au, Ag, Ir, Pt, Pd, Rh, or Ru stabilized by PVA (polyvinylacetate) were prepared by hydrogen reduction of the corresponding chloride salts [52]. Other organic polymers were used to stabilize metallic colloids. Rh, Pt, Pd, and Ir colloids are generated by using hydrogen as reducing agent in microemulsions [53,54].

3.3.1.3. Chemical Hydrides

The borohydrides ($NaBH_4$ or KBH_4) reduction of transition metal salts is the most widely used hydride reduction method of generating aqueous suspensions of metals. The stabilizing agents used in these cases are generally surfactants or water-soluble polymers. With this method Ru(0) nanoparticles were generated in the presence of acetate stabilizer [12]. Pt colloids were also stabilized by PVP (polyvinylpyrolidine) with this method [55].

Recently, $NaBH_4$ reduction was used to obtain Au, Ag, Pt, Pd, or Cu nanoparticles stabilized by dendrimers (polyamidoamine or PAMAM) [56,57,58]. These macromolecules allow one to obtain nearly monodispersed particles. Dimethylamineborane has been also used to prepare gold nanoparticles stabilized by hydrophobically modified PAMAM in toluene or chloroform.

Surfactants are generally used as stabilizers of aqueous colloidal suspensions of transition metal reduced by $NaBH_4$ or KBH_4. They can be cationic, anionic, or nonionic. In fact, Nakao and co-workers described the preparation of Ru, Rh, Pd, Pt, Ag, or Au nanoparticles stabilized by quaternary ammonium, sulfates, or poly(ethylene glycol) [59].

3.3.2. Thermolysis

Since many organometallic compounds of transition metals decompose thermally to their respective metals under relatively mild conditions, these compounds provide a rich source of nanoparticle precursors. The method is widely applicable. The thermolysis of carbonyl-containing complexes of rhodium, iridium, ruthenium, osmium, palladium, and platinum in polymer solutions has been used to prepare polymer-stabilized collodial metals with particle sizes in he range 1-10 nm, possibly by decomposition of polymer-bound organometallic intermediates [60].

Organols of palladium and platinum [61,62] have been synthesized by the thermolysis of precursors such as palladium acetate, palladium acetylacetonate, and platinum acetylacetonate in high boiling organic solvents such as methylisobuthyl ketone. These preparations have been performed in the absence of stabilizing polymers, and as a result relatively broad size distributions and large particles have been observed.

3.3.3. Photolysis and Radiolysis

Photochemical colloidal syntheses fall into two categories: the reduction of metal salts by radiolytically produced reducing agents such as solvated electrons and free radicals, and the photolysis of photolabile metal complexes. Again, the essence of the preparative procedure is the generation of zerovalent metal under conditions which prevent or at least retard the formation of bulk metal precipitates.

An advantage of radiolytic methods of colloidal metal synthesis lie in the fact that a large number of metal nuclei are produced homogeneously and instantaneously, a condition favorable for the formation of very highly dispersed particles [28].

3.3.4. Displacement of Ligands From Organometallic Complexes

Reduction of metal can be carried out prior to colloid preparation, giving a zerovalent metal complex as the immediate colloid precursor. The synthesis of metal carbonyls and their subsequent thermolysis in nanoparticles synthesis is an example of this approach. The zero-valent palladium and platinum complexes with dibenzylideneacetone $Pd(dba)_2$ and $M_2(dba)_3$ (M = Pd, Pt) have been known since 1970 to react under mild conditions with either hydrogen or carbon monoxide with the formation of metal [63].

3.3.5. Reduction by Electrochemical Methods

This large-scale synthetic procedure allows one to obtain size-controlled particles. A sacrificial anode is used as a metal source. This anode is oxidized in the presence of stabilizer, acting both the electrolyte and the stabilizing agent. The ions are then reduced at the cathode to yield the metallic nanoparticles. The proposed mechanism consists of (i) dissolution of the anode to form metal ions, (ii) migration of the metal ions to cathode, (iii) reduction of the metal ions at the surface of the cathode, (iv) aggregation of the particles by stabilizing agent around the metal cores then (v) precipitation of the metal nanoparticles.

3.4. Characterization of Metal Nanoparticles

The properties of colloidal metal nanoparticles that are of interest include size, structure and composition. The most widely used technique for characterizing nanoparticles is transmission electron microscopy (TEM) or high resolution transmission electron microscopy (HRTEM), which provides direct visual information of the size, dispersity, structure and morphology of nanoparticles. Other commonly used methods for characterization of metal particles include UV-Visible spectroscopy (UV-Visible), nuclear magnetic resonance spectroscopy (NMR), infrared spectroscopy (IR), elemental analysis, and energy dispersive spectroscopy (EDS). To a less extent the following methods are used; analytical ultracentrifugation-sedimentation, extended X-ray absorption fine structure (EXAFS), scanning tunneling microscopy (STM), atomic force microscopy (AFM), high performance liquid chromatography (HPLC), light scattering, time of flight mass spectroscopy, magnetic susceptibility and electrophoresis or ion-exchange chromatography. Figure 3.4 gives an overall picture of the methods most commonly used in the characterization of nanoparticles [64].

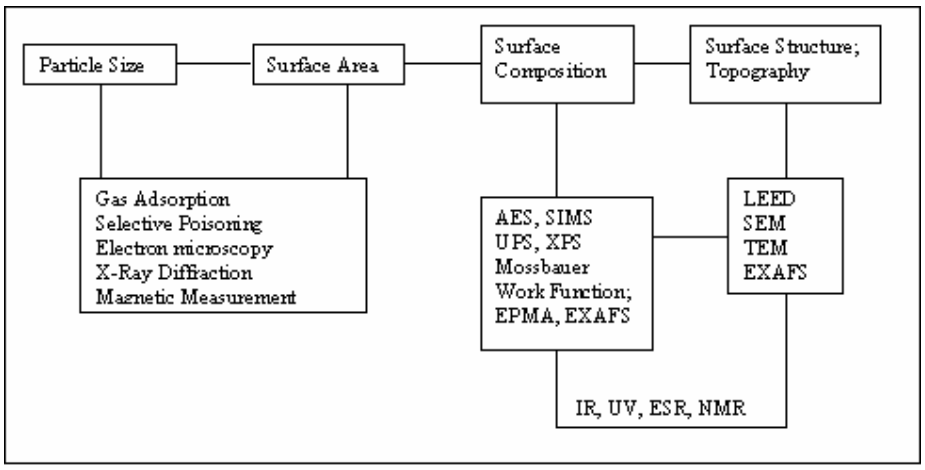

Figure 3.4 : Common methods available for nanoparticles characterization

CHAPTER 4

CATALYSIS

4.1. General Principles of Catalysis

It has long been known that the rates of many chemical reactions can be affected by traces of alien material which may be adventitiously present in the system or may be added deliberately. The word 'alien' is used to imply that the material it describes does not appear in stoichiometric equation for the reaction. Such a material is termed as a *catalyst* and it is define as a substance which increases the rate at which a chemical reaction approaches equilibrium, without being consumed in the process. The phenomenon occurring when a catalyst acts is termed *catalysis*. Catalysts are classified as *homogenous* when the catalyst is of the same phase as reactant and no phase boundary exist. However, when a phase boundary does separate the catalyst from the reactants, we speak of *heterogeneous* catalyst. There is however one extremely important group of substances which cannot be accommodated within this classification. *Enzymes* are neither homogenous nor heterogeneous catalysts; they are large, complex organic molecules, usually containing a protein.

The primary effect of a catalyst on a chemical reaction is, as stated in the above definition of catalysis, to increase its rate: this means therefore to increase its rate coefficient. The consequent effects may be analyzed in terms of transition-state theory. In the transition state theory, the effect of catalyst must be a decrease in the free energy of activation of the reaction. This, in turn, is composed of changes in entropy and enthalpy of activation. The entropy of activation in a catalyzed reaction will usually be less than in corresponding uncatalyzed reaction

because the transition state is immobilized on the catalyst surface with consequent loss of translational freedom. There must therefore be a corresponding decrease in the enthalpy of activation to compensate for this, or to overcompensate for efficient catalysis. Thus, according to the theory the activation energy for a catalyzed reaction ought to be less than for the same uncatalyzed reaction.

4.2. Energetics

A catalyst reduces the activation energy for both forward and backward reactions shown Figure 4.1, leaving the equilibrium position unchanged. For example when the reaction in Eq. 2;

$$2HI\ (g) \rightleftharpoons H_2(g) + I_2(g) \qquad \textbf{(2)}$$

is uncatalysed, its activation energy is 185 kJ mol^{-1} in the forward direction and 164 kJ mol^{-1} in the reverse direction. The activation energy in the forward direction is reduced to 59 $kJ.mol^{-1}$ when a platinum catalyst is used [65].

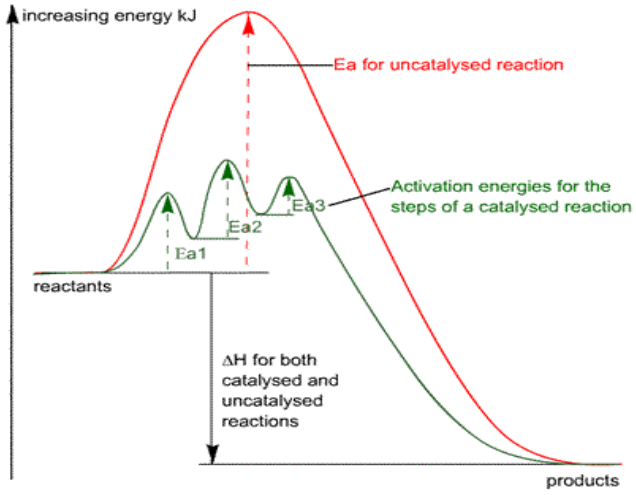

Figure 4.1 : Schematic representation of the energetics in a catalytic cycle.

A catalyst changes the activation energy of a reaction in two ways. In the first way, it forms bonds with one or more of the reactants and so reduces the energy needed by the reactant molecules in order to complete the reaction. In the second way, it brings the reactants together and holds them in a way that makes reaction more likely. When molecules come together in the appropriate orientation for reaction there is a big reduction in entropy. If a catalyst already holds the molecules next to each other then the entropy change for the reaction step will be far less negative than it would be without the catalyst, and the reaction is more likely. Note that the catalyst does not affect the overall entropy change for the reaction. In other words catalysts change the path of a reaction; they change its mechanism.

4.3. Properties of Catalysts

4.3.1. Catalytic Efficiency

The turnover frequency, *N*, is often used to express the efficiency of a catalyst. For the conversion of A to B catalyzed by Q and with a rate ν, Eq.3

$$A \xrightarrow{Q} B \quad v = \frac{d[B]}{dt} \tag{3}$$

the turnover frequency is given by the equation (4), (|Q| is mole of the catalyst)

$$N = \frac{v}{|Q|} \tag{4}$$

if the rate of the uncatalyzed reaction is negligible. A highly active catalyst, one that results in a fast reaction even in low concentrations, has a large turnover frequency.

The catalytic turnover number (TON) is the number of moles of product per mole of catalyst; this number indicates the number of catalytic cycles for a given process. The catalytic turnover frequency (TOF) is the catalytic turnover number per unit time: the number of moles of product per mole of catalyst per unit time.

In heterogeneous catalysis, the reaction rate is expressed in terms of the rate of change in the amount of product (in place of concentration), and the concentration of the catalyst replaced by the amount present. The determination of the number of active sites in a heterogeneous catalyst is particularly challenging, and often the denominator $|Q|$ in equation 4 is replaced by the surface area of the catalyst.

4.3.2. Selectivity

A selective catalyst yields a high proportion of the desired product with minimum amount of the side products. In industry, there is considerable economic **incentive** to develop selective catalysts. For example, when metallic silver is used to catalyze the oxidation of ethene with oxygen to produce ethylene oxide, the reaction is accompanied by the more thermodynamically favored but undesirable formation of CO_2 and H_2O. This lack of selectivity increases the consumption of ethane, so chemists are constantly trying to devise a more selective catalyst for this reaction.

4.3.3. Importance of Size Reduction of Catalysts

Surface chemistry is of vital importance in numerous processes, including corrosion, adsorption, oxidation-reduction and catalysis. Particles in the 1-10 nm range open a new vista in surface chemistry because surface-reactant interactions can become stoichometric, this is due to two reasons. First, the huge surface areas

of the nanostructured material dictate that many of the atoms are on the surface, thus allowing good 'atom economy' in surface-gas, surface-liquid, or even surface-solid reactions. Figure 4.2 illustrates the calculated numbers of iron atoms on spherical iron nanoclusters that are surface or bulk atoms.

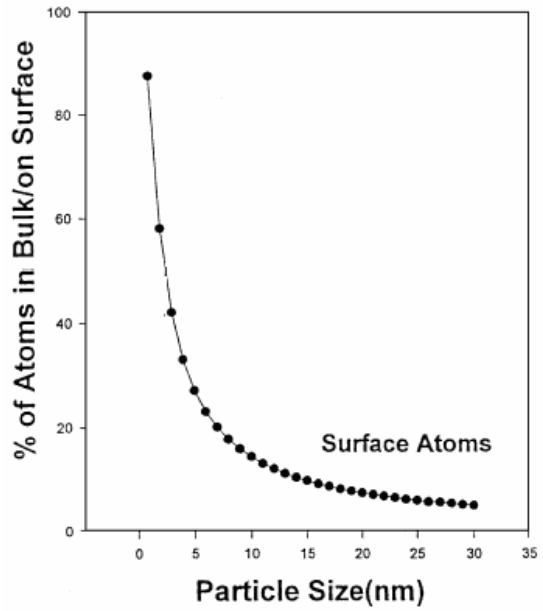

Figure 4.2. Calculated surface to bulk atom ratios for spherical iron nanoparticles (Adapted from the reference[66]).

Note that quite small sizes are necessary; indeed, a 3 nm particle has 50% of the atoms on the surface, while a 20 nm particle has fewer than 10%. This demonstrates that it is necessary to get small particles in order to benefit from the atom economy desired. Features of the nanoclusters are enhanced intrinsic chemical reactivity as size gets smaller. The increasing proportion of surface atoms with decreasing particle size, compared with bulk metals, makes small metal particles become highly reactive catalysts, as surface atoms are the active centers for catalytic elementary processes. Among the surface atoms, those sitting on the edges and corners are more active than those in planes.

The percentage of edge and corner atoms also increases with decreasing size and this is why very small particles are preferred as catalyst. Figure 3.3 shows this effect clearly.

Full-shell Clusters		Total Number of Atoms	Surface Atoms (%)
1 Shell		13	92
2 Shells		55	76
3 Shells		147	63
4 Shells		309	52
5 Shells		561	45
7 Shells		1415	35

Figure 4.3. The relation between the total number of atoms in full shell clusters and the percentage of surface atoms.

Among the chemical properties of transition metal nanoclusters discussed above, catalysis is of great interest because of their high surface to volume ratio and a unique combination of reactivity, stability, and selectivity.

CHAPTER 5

EXPERIMENTAL

5.1. Materials

Nickel(II) acetylacetonate (95%), sodium borohydride (98%) were purchased from Aldrich® and sodium phosphate ($Na_3PO_4 \cdot 12H_2O$) was purchased from Riedel-De Haen AG Hannover. Deionized water was distilled by water purification system (Şimşek SL-200, Ankara, Turkey). All glassware and Teflon coated magnetic stirring bars were cleaned with acetone, followed by copious rinsing with distilled water before drying in an oven at 150 ^oC.

5.2. In-situ formation of hydrogenphosphate-stabilized nickel(0) nanoclusters and catalytic hydrolysis of sodium borohydride

In-situ formation of hydrogenphosphate-stabilized nickel(0) nanoclusters and catalytic hydrolysis of sodium borohydride were performed in the same medium. Before starting the experiment, a jacketed reaction flask (75 mL) containing a Teflon-coated stirring bar was placed on a magnetic stirrer (Heidolph MR-301) and thermostated to 25.0 ± 0.1 °C by circulating water through its jacket from a constant temperature bath (Lauda RL6). Then, a graduated glass tube (50 cm in height and 4.7 cm in diameter) filled with water was connected to the reaction flask to measure the volume of the hydrogen gas to be evolved from the reaction. Next, 284 mg (7.47 mmol) $NaBH_4$ (corresponding to 30 mmol = 672 mL H_2 at 25.0 ± 0.1 °C and 0.91 atm pressure) and 26.6 mg (0.07 mmol) $Na_3PO_4.12H_2O$ were dissolved in 40 mL water. The solution was transferred with

a 50 mL glass-pipette into the reaction flask thermostated at 25.0 ± 0.1 °C. Then, 10 mL aliquot of 7.0 mM nickel(II) acetylacetonate solution was transferred into the reaction flask using a 10 mL gastight syringe and the solution was stirred at 1200 rpm. The initial concentrations of $NaBH_4$ and nickel(II) acetylacetonate were 150 mM (7.5 mmol) and 1.4 mM (0.07 mmol), respectively. A molar ratio of $NaBH_4$ to $Ni(acac)_2$ greater than 100 was used to ensure complete reduction of Ni^{+2} to its zero oxidation state and to observe the catalytic hydrolysis of sodium borohydride at the same time. A fast color change from pale green to dark brown was observed indicating the formation of nickel(0) nanoclusters. When the nanoclusters formation was completed (within less than 1 minute) the catalytic hydrolysis was started to be measured by monitoring the volume of hydrogen gas evolved. The volume of hydrogen gas evolved was measured by recording the displacement of water level every 5 minutes at constant pressure. The reaction was stopped when 75% conversion was achieved. No bulk metal formation was observed during the catalytic hydrolysis reaction. The pH of the solution was measured during the reaction by using a Fischerbrand pH meter.

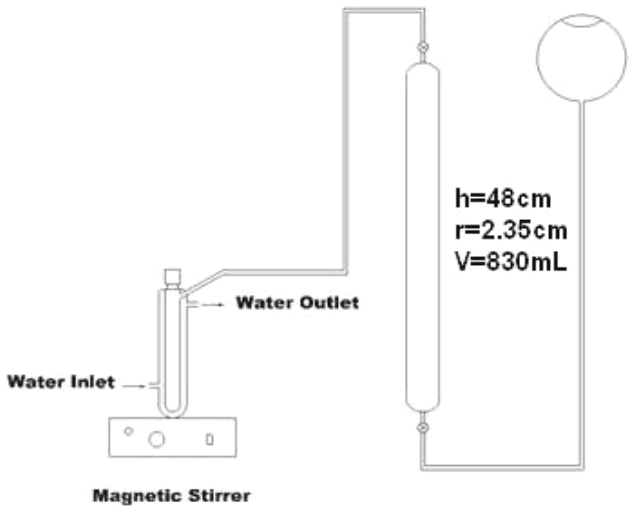

Figure 5.1. The experimental setup used in performing the catalytic hydrolysis of sodium borohydride and measuring the hydrogen generation rate.

5.3. Self-Hydrolysis Of Sodium Borohydride

In a 100 mL beaker, 284 mg (7.47 mmol) sodium borohydride was dissolved in 2 mL water and the volume of the solution was adjusted to 50 mL by adding water. The solution was then transferred with a pipette into the reaction flask thermostated at 25.0 ± 0.1 °C. The experiment was started by closing the reaction flask and turning on the stirring at 1200 rpm simultaneously, exactly in the same way as described in the previous section. The volume of hydrogen gas generated was measured every 5 minutes. The pH of the solution was measured during the reaction by using a Fisherbrand Hydrus 500 pH meter.

5.4. Kinetic Study Of Hydrogenphsphate-Stabilized Nickel(0) Nanocluster In Catalytic Hydrolysis Of Sodium Borohydride

In order to establish the rate law for catalytic hydrolysis of $NaBH_4$ using hydrogenphosphate-stabilized nickel(0) nanoclusters, two different sets of experiments were performed in the same way as described in the section "In-situ formation of hydrogenphosphate-stabilized nickel(0) nanoclusters and catalytic hydrolysis of sodium borohydride". In the first set of experiments, the hydrolysis reaction was performed starting with different initial concentration of nickel(II) acetylacetonate (1.0, 1.2, 1.4, 1.6, 1.8, 2.0 mM) and keeping the initial sodium borohydride concentration constant at 150 mM. The second set of experiments were performed by keeping the initial concentration of nickel(II) acetylacetonate constant at 1.4 mM and varying the $NaBH_4$ concentration to provide a substrate to catalyst ratio of 150, 300, and 450. Finally, the catalytic hydrolysis of $NaBH_4$ was performed in the presence of Ni(0) nanoclusters at constant substrate (150 mM) and catalyst (1.4 mM) concentrations at various temperatures in the range of 25-45 °C in order to obtain the activation energy (E_a), enthalpy ($\Delta H^{\#}$), and entropy ($\Delta S^{\#}$).

5.5. Effect Of Hydrogenphosphate Concentration On The Catalytic Activity Of Nickel(0) Nanoclusters

In order to study the effect of hydrogenphosphate concentration on the catalytic activity of nickel(0) nanoclusters in the hydrolysis of sodium borohydride (150 mM), catalytic activity tests were performed at 25.0 ± 0.1 °C starting with various concentrations of sodium phosphate (0.5, 0.8, 1.0, 1.5, 2.0 and 10 M) in the in-situ generation of nickel(0) nanoclusters. In all the experiments the total volume of solution was kept constant at 50 mL. All the experiments were performed in the same way as described in the section "In-situ formation of hydrogenphosphate-stabilized nickel(0) nanoclusters and catalytic hydrolysis of sodium borohydride".

5.6. Catalytic Lifetime Of Hydrogenphosphate-Stabilized Nickel(0) Nanoclusters

The catalytic lifetime of hydrogenphosphate stabilized-nickel(0) nanoclusters in the hydrolysis of sodium borohydride was determined by measuring the total turnover number (TON). Such a lifetime experiment was started with a 50 mL solution containing 0.8 mM nickel(II) acetylacetonate and 450 mM $NaBH_4$ (corresponding to maximum possible total turnover number of 2250) at 25.0 ± 0.1 °C. The nanocluster formation and hydrolysis of sodium borohydride reaction was continued until hydrogen gas evolution was slowed down to the self hydrolysis level.

5.7. Characterization of Hydrogenphosphate-Stabilized Nickel(0) Nanoclusters

5.7.1. XPS (X-Ray photoelectron spectroscopy)

XPS Sample Preparation; After catalysis, described in the previous section, 10 mL aliquots of hydrogenphosphate-stabilized nickel(0) nanoclusters solution were transferred via a disposable pipette into eight new 15×100 mm glass tubes separately and all the samples were simultaneously centrifuged (Heraeus Labofuge 200) with 3500/min stirring rate for 4 hours. After the decantation of the supernatant solution, the precipitates were dried under vacuum for 2 hours. The dry samples of nickel(0) nanoclusters were collected in a screw-capped glass vial and sent to the METU Central Laboratory for XPS analysis.

XPS Analysis; X-ray photoelectron spectrum (XPS) was taken at the Middle East Technical University Central Laboratory using SPECS spectrometer equipped with a hemispherical analyzer and using monochromatic Mg-Kα radiation (1250.0 eV, the X-ray tube working at 15 kV and 350 W) and pass energy of 48 eV.

5.7.2. Powder XRD (X-Ray Diffraction)

The sample prepared for the XPS analysis was also used for taking the powder X-ray diffraction pattern. Powder X-ray diffraction pattern of hydrogenphosphate-stabilized nickel(0) nanoclusters was taken on Rigaku Miniflex XRD with CuKα radiation source (30 kV, 15 mA, 1.54 Å).

5.7.3. FT-IR Spectra

The sample prepared for the XPS analysis was also used for taking the FTIR spectra. FTIR spectrum of the hydrogenphosphate-stabilized nickel(0) nanoclusters was taken from KBr pellet on a Bruker FRA 20 FTIR Spectrophotometer using Opus software.

5.7.4. UV Spectra

In two glass vials, 10 mL aqueous solution of 0.14 mM $Ni(acac)_2$ (pale green in color) and 10 mL of aqueous solution of 1.4 mM $NaBH_4$ and 0.14 mM $Na_3PO_4.12H_2O$ mixture were prepared separately. Absorbance at 294 nm was followed by using rapid-mix technique combined with a Hewlett Packard 8452A Model Diode Array Spectrophotometer with kinetics program of UV-Visible ChemStation software. The electronic absorbance spectra were taken every two seconds under pseudo-first order conditions. Thus, the reduction of nickel(II) acetylacetonate could be followed.

5.8. Mercury Poisoning Of Hydrogenphosphate-Stabilized Nickel(0) Nanoclusters

In a poisoning experiment, hydrogenphosphate-stabilized nickel(0) nanoclusters generated from the reduction of nickel(II) acetylacetonate (7.0 mmol) in 50 mL of 150 mM sodium borohydride solution in the presence of 6.0 mM HPO_4^{-2} ion at 25.0 ± 0.1 °C was poisoned by using 60, 30, 12, 6.0, 3.0, and 2.4 mg mercury corresponding to a Hg/Ni molar ratio of 0.1, 0.08, 0.06, 0.04, 0.02 and 0.01, respectively. The catalytic activity was measured by monitoring the rate of hydrogen generation before and after the addition of mercury.

5.9. Isolability and Redispersibility of Hydrogenphosphate-Stabilized Nickel(0) Nanoclusters

The samples of hydrogenphosphate-stabilized nickel(0) nanoclusters prepared as described above were centrifuged (Heraeus Labofuge 200) and rinsed twice with a 30% (v/v) water/ethanol mixture. The residue was dried under vacuum. Then, the isolated nickel(0) nanoclusters were redispersed in 50 mL aqueous solution of 150 mM sodium borohydride and their catalytic activities were tested exactly in the same way as in the section "In-situ formation of hydrogenphosphate-stabilized nickel(0) nanoclusters and catalytic hydrolysis of sodium borohydride".

CHAPTER 6

RESULTS AND DISCUSSION

6.1. In-Situ Formation Of Hydrogenphosphate-Stabilized Nickel(0) Nanoclusters and Catalytic Hydrolysis Of Sodium Borohydride

Nickel(0) nanoclusters can be in-situ generated from reduction of nickel(II) acetylacetonate by sodium borohydride in aqueous solution and stabilized by HPO_4^{2-} anion. Hydrogenphosphate-stabilized nickel(0) nanoclusters, dark brown in color, were found to be stable in aqueous media. No precipitation observed during the catalytic hydrolysis of sodium borohydride. These hydrogenphosphate-stabilized nickel(0) nanoclusters act as a catalyst in the hydrolysis of sodium borohydride as well.

6.2. Effect Of Hydrogenphosphate Concentration On The stability and activity of Nickel(0) Nanoclusters Catalyst

The effect of the stabilizer concentration on the stability and catalytic activity of the nickel(0) nanoclusters catalyst was investigated by performing the catalytic hydrolysis of sodium borohydride starting with 1.4 mM nickel(II) ion and different hydrogenphosphate ion concentration. Figure 6.1 shows the volume of hydrogen generated versus time plot for the hydrolysis of sodium borohydride catalyzed by nickel(0) nanoclusters, using different concentrations of hydrogenphosphate ion at 25.0 ± 0.1 °C.

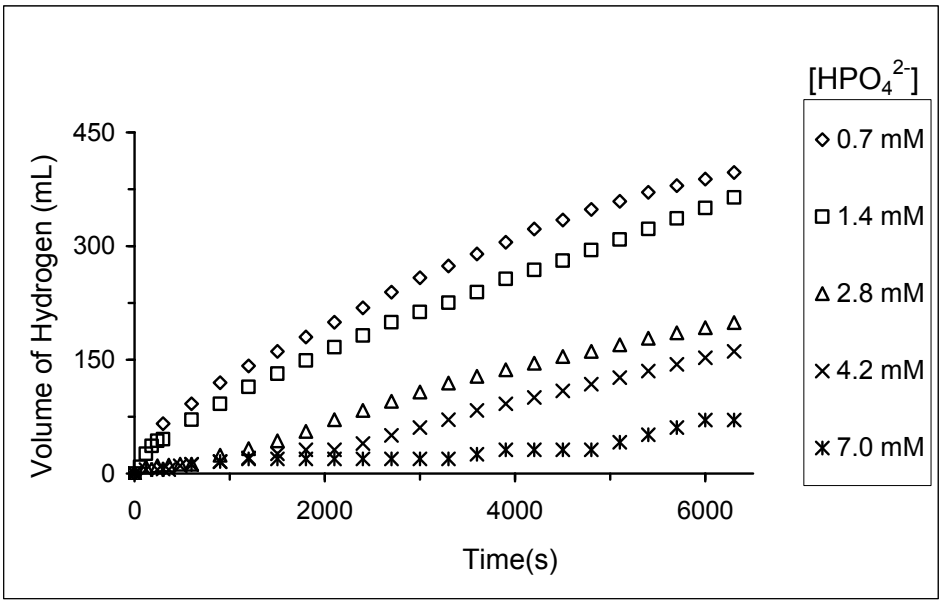

Figure 6.1. The graph of volume of hydrogen versus time for the hydrolysis of sodium borohydride catalyzed by nickel(0) nanoclusters starting with various hydrogenphosphate concentrations at 25 ± 0.1 °C. [Ni] = 1.4 mM, [$NaBH_4$] =150 mM .

Rapid hydrogen generation starts immediately without induction period at hydrogenphosphate concentration equal to or lower than 1.4 mM. The hydrogen generation continues almost linearly and then slows down as the substrate concentration decreases toward the end of reaction. At hydrogenphosphate concentrations equal to or higher than 2.8 mM, an induction period of 5-30 minutes is observed. Figure 6.2 shows that the hydrogen generation rate, measured from the nearly linear portion of the curves in Figure 6.1, decreases with the increasing concentration of hydrogenphosphate. This indicates that the catalytic activity of nickel(0) nanoclusters decreases with the increasing concentration of stabilizer as expected [67].

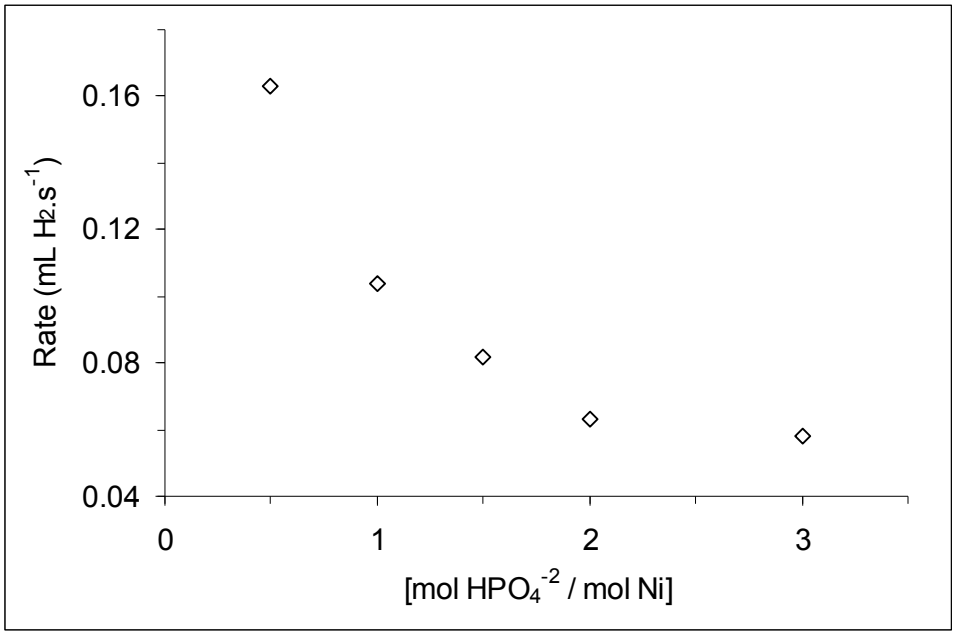

Figure 6.2. The rate of hydrogen generation versus the molar ratio of hydrogenphosphate to nickel.

While no precipitation of bulk nickel was observed during the catalytic hydrolysis of sodium borohydride in the presence of hydrogenphosphate ion in concentrations higher than 1.4 mM, abrupt formation of bulk nickel was observed after 20 minutes of catalytic hydrolysis using hydrogenphosphate ion concentration of 0.7 mM. Thus, the hydrogenphosphate concentration of 1.4 mM, corresponding to a hydrogenphosphate to nickel ratio of 1, was selected for the further experiments.

6.3. Reduction of Nickel(II) Acetylacetonate by Sodium Borohydride

The absence of an induction period during the formation of nickel(0) nanoclusters starting with 1.4 mM nickel(II) acetylacetonate and 1.4 mM hydrogenphosphate ion implies that the reduction of nickel(II) acetylacetonate by sodium borohydride is fast. Indeed, standard UV-Visible spectroscopy could not

be used to follow the reduction of nickel(II) acetylacetonate in the presence of 1 fold hydrogenphosphate ion. However, using rapid-mix technique combined with a UV-visible spectrophotometer enables us to follow this fast reaction.

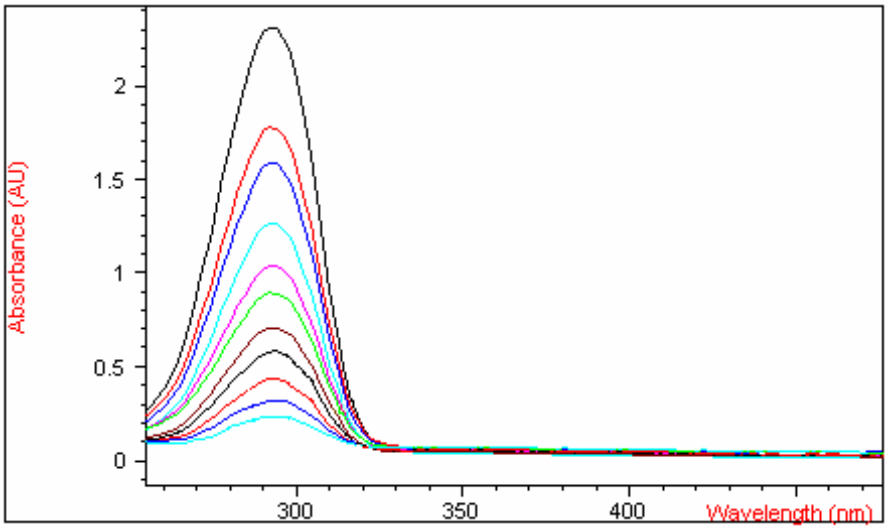

Figure 6.3. UV spectrum of reduction of nickel(II) acetylacetonate (0.14 mM) by sodium borohydride (1.4 mM) in aqueous solution at 25 °C.

Figure 6.3 shows changes in the UV-visible spectrum of an aqueous solution of nickel(II) acetylacetonate (0.14 mM) during the reduction reaction by sodium borohydride (1.4 mM) in the presence of 0.14 mM hydrogenphosphate ion at 25 °C. The spectral feature due to Ni^{2+} ion disappears almost completely within 70 s. The reaction obeys a pseudo first order kinetics with rate constant of $k = 7.0\times10^{-3}$ s^{-1}as shown by absorbance versus time plot at 294 nm in Figure 6.4.

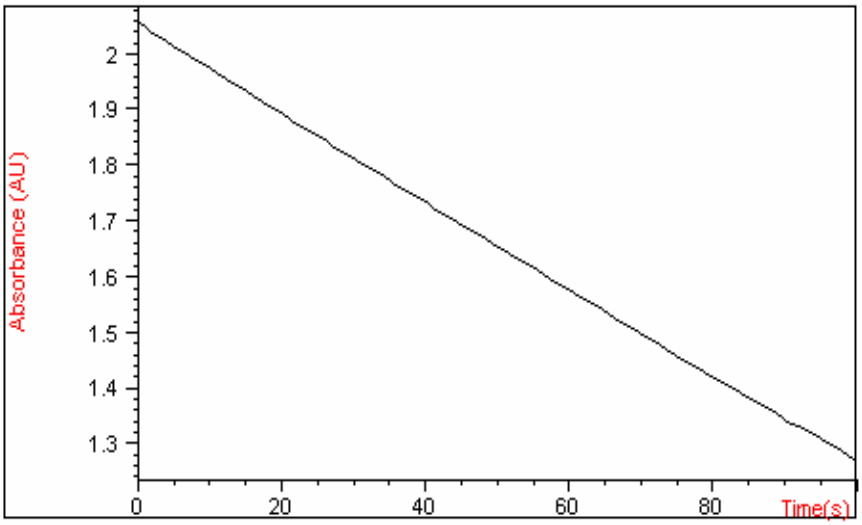

Figure 6.4. ln A versus Time(s) plot at 294 nm for the reduction of nickel(II) acetylacetonate (0.14 mM) by sodium borohydride (1.4 mM) in aqueous solution at 25°C.

The formation of nickel in zero oxidation state from reduction of nickel(II) acetylacetonate by sodium borohydride was also shown by XPS. Figure 6.5 shows the XPS spectrum of hydrogenphosphate-stabilized nickel(0) nanoclusters prepared in aqueous solution from the reduction of nickel(II) acetylacetonate (1.4 mM) by sodium borohydride (150 mM) in the presence of hydrogenphosphate (1.4 mM) at 25 ± 0.1 °C.

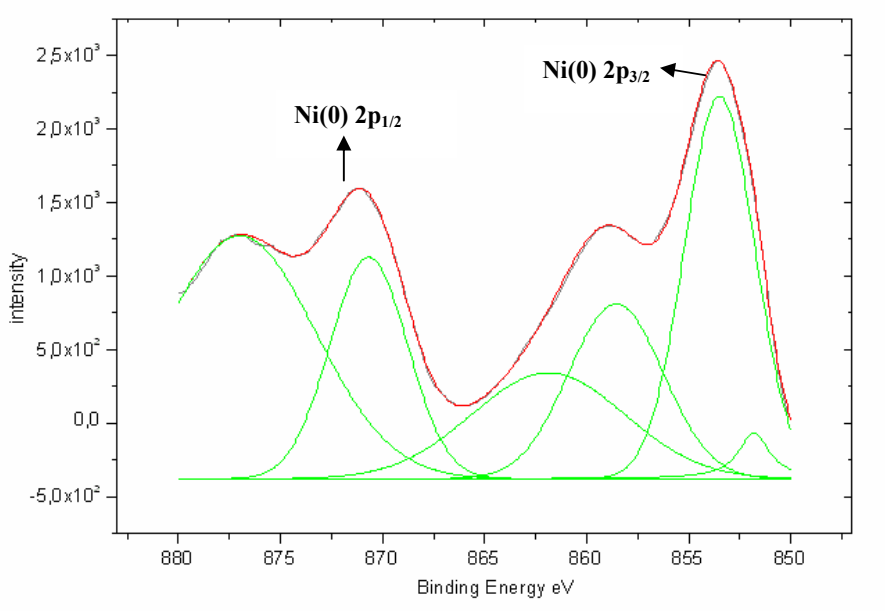

Figure 6.5. X-Ray photoelectron spectrum of hydrogenphosphate-stabilized nickel(0) nanoclusters prepared in aqueous solution from the reduction of nickel(II) acetylacetonate (1.4 mM) by sodium borohydride (150 mM) in the presence of hydrogenphosphate (1.4 mM) at 25 ± 0.1 °C.

The XPS spectrum in Figure 6.5 exhibits two bands at 853.6 and 871 eV which can be assigned to Ni(0) $2p_{3/2}$ and Ni(0) $2p_{1/2}$, respectively. Compared to the values for the bulk nickel (852.3 and 869.7 eV, respectively) [68], the $2p_{3/2}$ and $2p_{1/2}$ binding energies are slightly shifted to the higher values which can be attributed to the matrix effect [69]. The XPS spectrum shows two additional higher energy bands 858.5 and 877.5 eV, though with relatively weak intensities. These bands can be attributed to Ni(II) $2p_{3/2}$ and Ni(II) $2p_{1/2}$, respectively [68]. Ni(II) species might have been formed during the XPS sample preparation, since the hydrogenphosphate-stabilized nickel(0) nanoclusters are sensitive to aerobic atmosphere.

The average size of hydrogenphosphate-stabilized nickel(0) nanoclusters was estimated from the powder X-ray diffraction patern. Figure 6.6 shows the powder XRD pattern of hydrogenphosphate-stabilized nickel(0) nanoclusters prepared in aqueous solution from the reduction of nickel(II) acetylacetonate (7 mM) by sodium borohydride (150 mM) in the presence of hydrogenphosphate (7 mM) at 25 ± 0.1 °C.

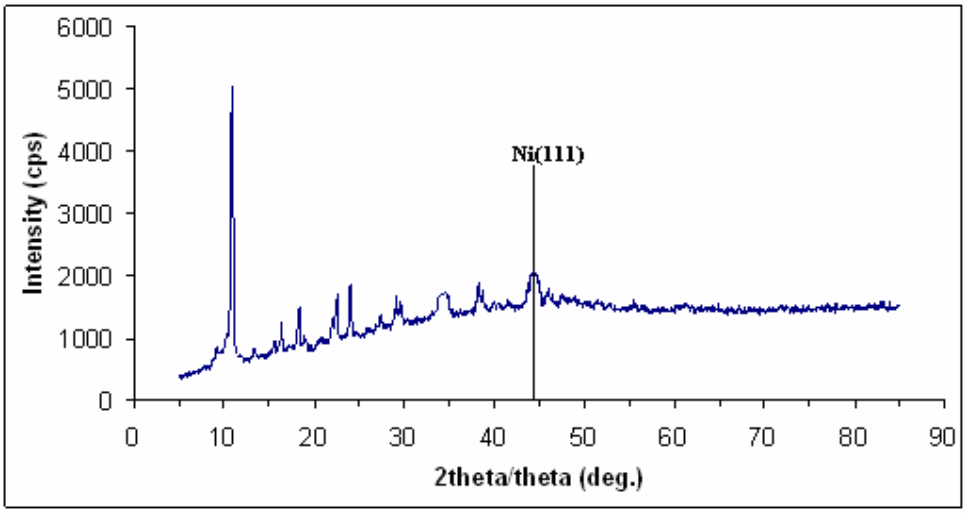

Figure 6.6. Powder XRD spectrum of hydrogenphosphate-stabilized nickel(0) nanoclusters

The broad peak at $2\theta = 44.5^{o}$ indicates (111) planes of nickel as compared with values given in the catalog (04-0850) for nickel ($2\theta(111) = 44.507$) According to literature [70], the size of nanoparticles can be estimated from their powder X-ray diffraction patterns by using Debye-Scherrer equation shown in equation 5;

$$L = \frac{0.9\lambda}{B\cos\theta} \qquad \textbf{(5)}$$

L is the coherence length, λ is the wavelength of x-ray radiation, B is the full width at half-maximum and θ is the angle of reflection of the peak. The average particle size of the hydrogenphosphate-stabilized nickel(0) nanoclusters was estimated 8.8 ± 2 nm from the half-width of the intense 111 reflection by the use of Debye-Scherrer equation.

6.4. Integrity of Hydrogenphosphate Stabilizer

Integrity of hydrogenphosphate stabilizer was examined by FTIR and ^{31}P-NMR spectroscopy. FTIR spectra of the isolated hydrogenphosphate-stabilized nickel(0) nanoclusters and that of the hydrogenphosphate ion in $Na_2HPO_4.7H_2O$ are displayed together in Figure 6.7.

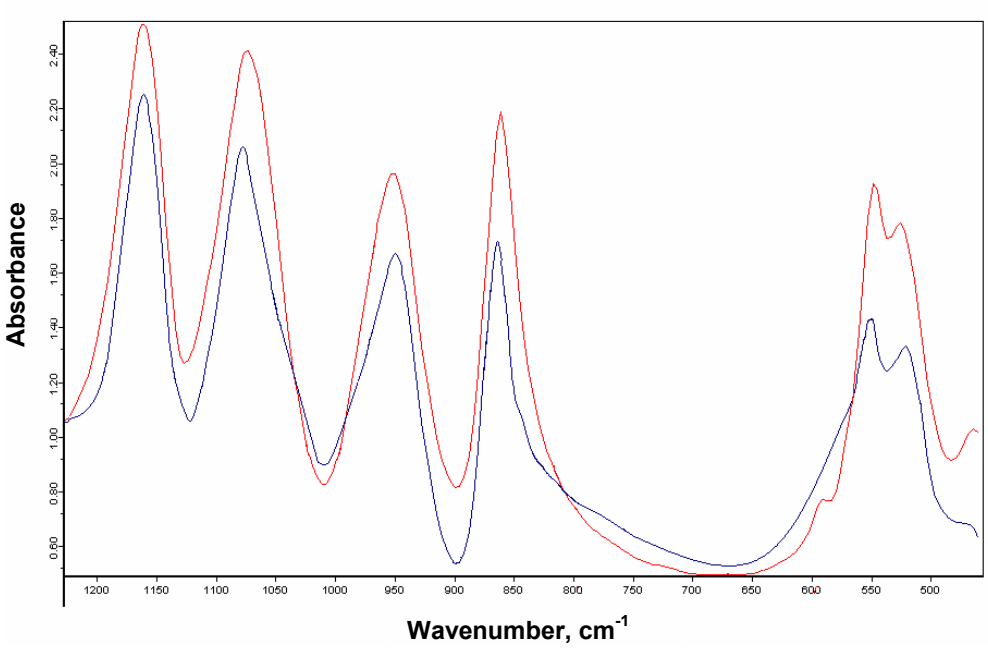

Figure 6.7. FT-IR spectrum of isolated hydrogenphosphate-stabilized nickel(0) nanoclusters (bottom curve) and free hydrogenphosphate anion (upper curve)

The hydrogenphosphate ion in $Na_2HPO_4.7H_2O$ has characteristics bands at **1000-1100 cm^{-1}.** The comparison of IR spectra of free hydrogenphosphate and isolated hydrogenphosphate-stabilized nickel(0) nanoclusters shows that hydrogenphosphate ions exist in the nanoclusters sample most probably on the surface of particles.

The ^{31}P-NMR spectrum gives the same signal at 2.05 ppm for both the solution of sodium hydrogenphosphate and reaction solution after catalysis. This reveals that the hydrogenphosphate anion maintains its integrity during the nanocluster formation and catalysis.

6.5. Heterogeneity, Redispersibilty, and Lifetime of Catalyst

In order to determine of catalytically active sites on the surface of the hydrogenphosphate-stabilized nickel(0) nanoclusters, a series of mercury poisoning experiments were carried out by adding mercury in varying amount during the catalytic hydrolysis of sodium borohydride and measuring the catalytic activity before and after addition. Figure 6.8 shows the results of eight independent experiments as a plot of the relative rate of hydrogen generation versus the relative mercury concentration as moles of Hg/moles of nickel.

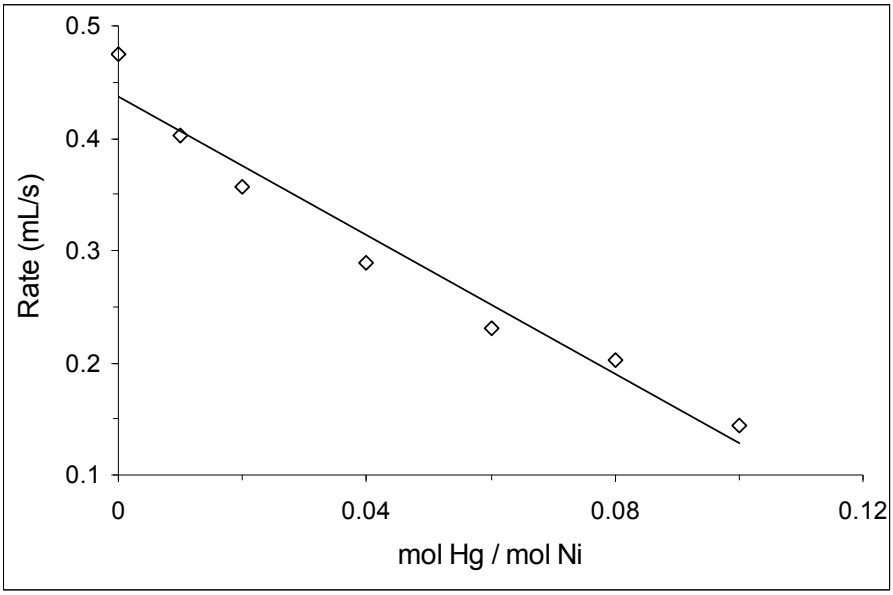

Figure 6.8. Rate versus mol Hg / mol Ni in different mercury concentration

Experimental points can be fitted to a line, the intersection of which with the concentration axis provides the critical molar ratio of mercury to nickel [71]. Thus, the minimum amount of mercury required for the complete poisoning of the nickel(0) nanoclusters catalyst was found to be 0.11 ± 0.05 mol of Hg / mol of total nickel. By assuming a 1/1 *Hg/Ni(0)* stoichiometry [72] for the poisoning, one obtains 11 % of the total nickel atoms to be active in catalysis.

Hydrogenphosphate-stabilized nickel(0) nanoclusters were isolated by centrifugation followed by drying in vacuum. These isolated nickel(0) nanoclusters were redispersed in water and tested for their catalytic activity in the hydrolysis of sodium borohydride after being stored for 1 day. The isolated nickel(0) nanoclusters could be easily dispersed in water and giving rise to a clear dark brown colloidal solution of nickel. After a day of storage, the sample prepared by redispersing the isolated nickel(0) nanoclusters was still found to be active catalyst in the hydrolysis of sodium borohydride.

The reaction rates indicate that hydrogenphosphate-stabilized nickel(0) nanoclusters retain 60 % of their catalytic activity in the hydrolysis of sodium borohydride, when isolated and redispersed in water.

A catalyst lifetime experiment was performed starting with 0.8 mM nickel(II) acetylacetonate nanoclusters and 450 mM sodium borohydride in 50 mL aqueous solution at 25.0 ± 0.1 °C, corresponding to a maximum total turnover number of 2250. It was found that the hydrogenphosphate-stabilized nickel(0) nanoclusters provide 1450 turnovers of hydrogen gas generation from the hydrolysis of sodium borohydride over 4 hours before deactivation. This corresponds to a turnover frequency of 6.04 min^{-1}.

6.6. Kinetics Of Hydrolysis Of Sodium Borohydride Catalyzed By Hydrogenphosphate-Stabilized Nickel(0) Nanoclusters

It is well known that $NaBH_4$ hydrolyzes to spontaneously give hydrogen gas in water. However, the hydrogen gas evolution rate is very slow compared to that the catalytic hydrolysis using nickel(0) nanoclusters as catalyst. For example, in the absence of a catalyst, the self hydrolysis of 50 mL of 150 mM sodium borohydride solution liberates 94 mL of H_2 gas in 1 hours while sodium borohydride liberates 450 mL H_2 gas in the presence of 1.4 mM nickel(0) nanoclusters in 1 hour at 25 ± 0.1 ^oC.

The hydrogenphosphate-stabilized nickel(0) nanoclusters are found to be active catalyst for the hydrolysis of sodium borohydride at low concentrations and room temperatures as shown in Figure 6.9, which plots the volume of hydrogen generated versus time during the catalytic hydrolysis of 150 mM $NaBH_4$ solution in the presence of nickel(0) nanoclusters in different concentrations at 25 ± 0.1 ^oC.

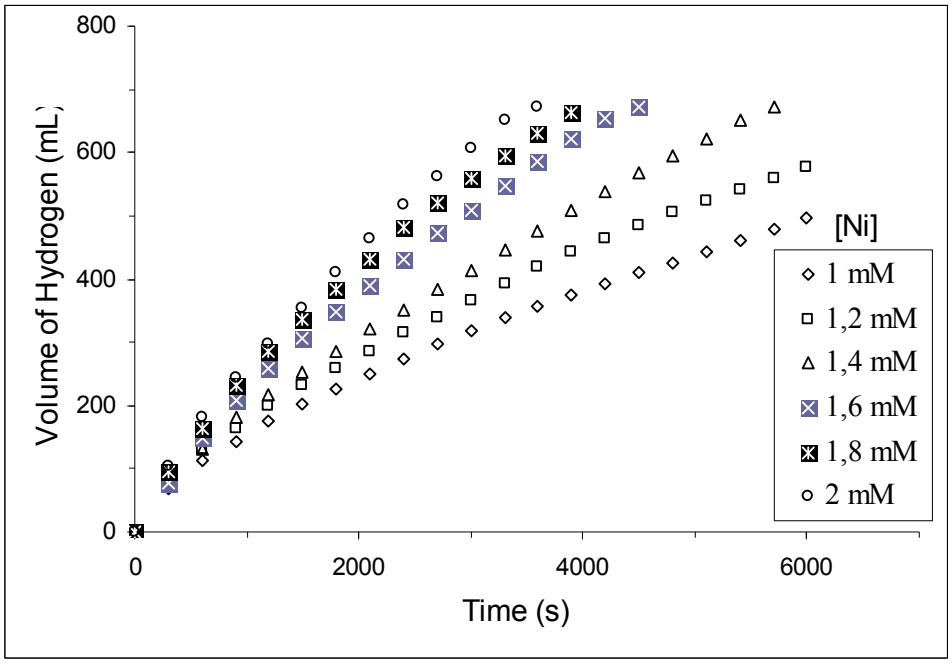

Figure 6.9. The graph of volume of hydrogen (mL) versus Time (s) in different Nickel(II) acetylacetonate concentrations in all sets [$NaBH_4$] = 150 mM

The hydrogen generation rate was determined from the nearly linear portion of the plot for each concentration of nickel(0) nanoclusters. Figure 6.10 shows the plot of hydrogen generation rate versus nickel(II) acetylacetonate concentration, both in logarithmic scale. The slope of which is found to be 1.11 ≈ 1.0 indicating that the hydrolysis reaction is first order with respect to the concentration of nickel(0) nanoclusters catalyst.

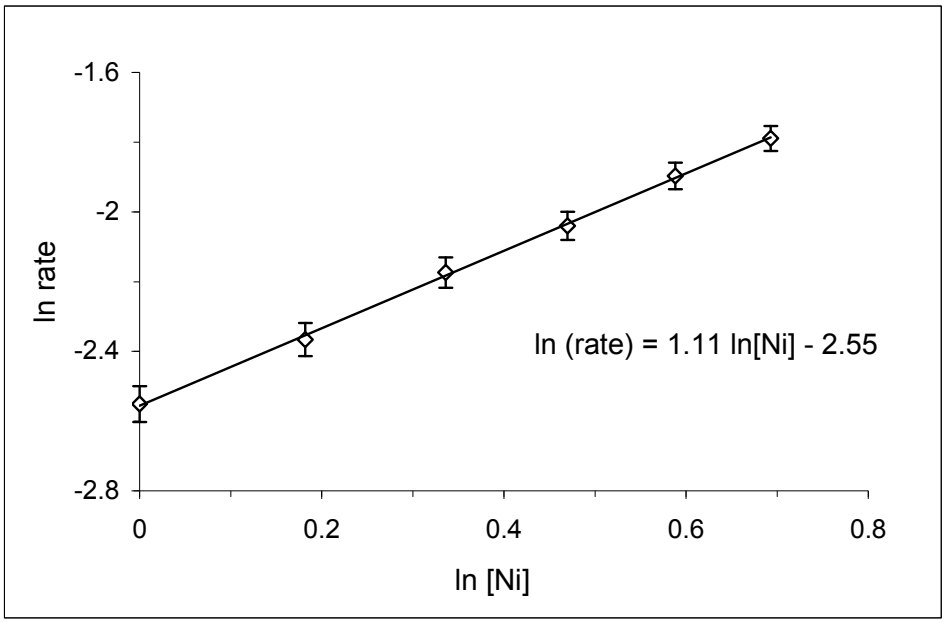

Figure 6.10. The graph of ln Rate versus ln [Ni] at 25 ^{o}C and 150 mM $NaBH_4$

The effect of $NaBH_4$ substrate concentration on the hydrogenation rate was also studied by performing a series of experiments starting with different initial concentration of $NaBH_4$ while keeping the catalyst concentration constant at 1.4 mM nickel(II) acetylacetonate. Figure 6.11 shows that the concentration of sodium borohydride decreases linearly as the reaction proceeds, starting with three different initial concentration of sodium borohydride but constant nickel(II) acetylacetonate concentration.

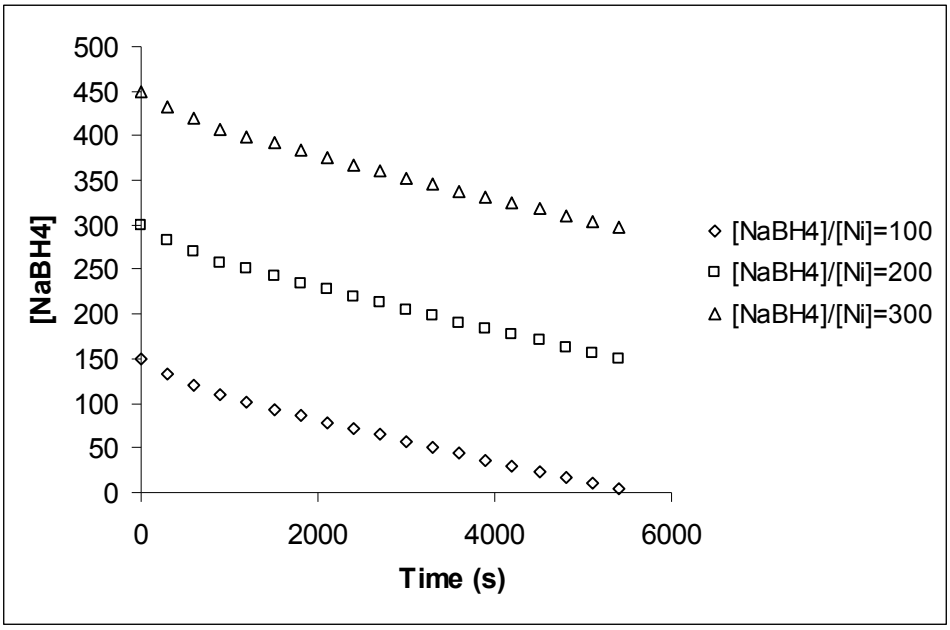

Figure 6.11. The graph of [$NaBH_4$] versus Time(s)

The slope of the line fitted to the experimental data shown in Fig. 6.12 is very small indicating that the hydrolysis reaction can be assumed to be zero order with respect to the concentration of $NaBH_4$.

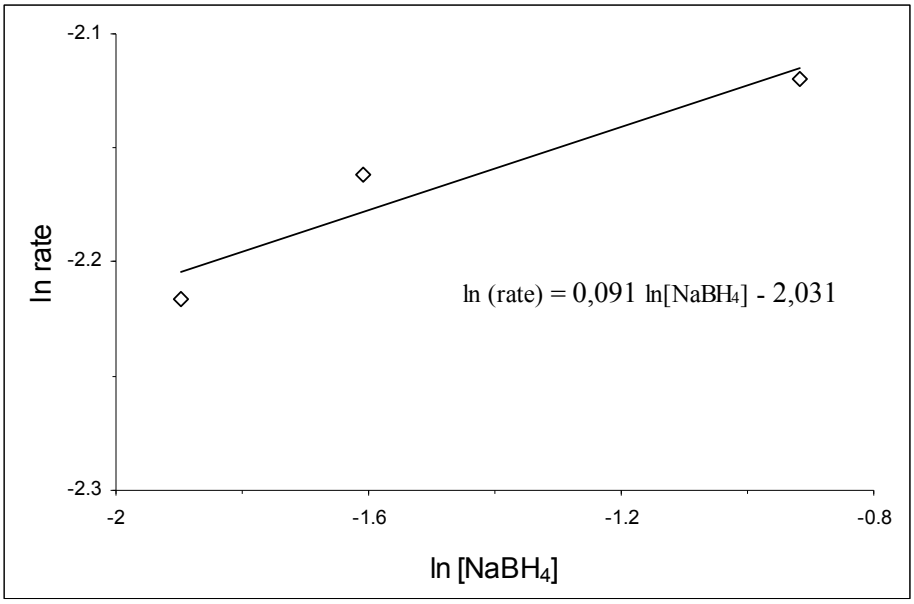

Figure 6.12. ln rate versus ln [$NaBH_4$] at constant [Ni]=1.4 mM

Thus, the rate law for the catalytic hydrolysis of sodium borohydride can be given as;

$$\frac{-4d[NaBH_4]}{dt} = \frac{d[H_2]}{dt} = k[Ni] \qquad \textbf{(6)}$$

Both nickel(0) nanoclusters catalyzed and self hydrolysis of sodium borohydride were carried out at various temperature in the range of 25-45 °C starting with the initial substrate concentration of 150 mM $NaBH_4$ and an initial catalyst concentration of 1.4 mM nickel(II) acetylacetonate. The values of rate constant were calculated by abstraction of self hydrolysis hydrogen generation values from those of nickel(0) nanoclusters catalyzed hydrolysis of sodium borohydride. They are listed in Table 6.1.

Table 6.1. Rate constants for the hydrolysis of sodium borohydride catalyzed by Ni(0) nanoclusters starting with a solution of 150 mM $NaBH_4$ and 1.4 mM Nickel(0) nanoclusters at different temperatures.

Temperature (^{0}C)	Rate Constant, k ($[NaBH_4].[mol\ Ni(0)]^{-1}.s^{-1}$)
25	0,05
30	0,08
35	0,112
40	0,163
45	0,212

The rate constant / temperature data was evaluated according to the Arrhenius equation and Eyring equation to obtain the activation energy, the activation enthalpy and entropy. First, the Arrhenius equation was used for the evaluation:

$$k = A.e^{-\frac{Ea}{RT}} \qquad \textbf{(7)}$$

where A and E_a are constants characteristics of the reaction and R is the gas constant. E_a is the Arrhenius activation energy and A is the pre-exponential factor [73]. Taking the natural logarithm of equation **7**, gives equation **8**:

$$\ln k = \ln A - \left(\frac{Ea}{RT}\right) \qquad \textbf{(8)}$$

Figure 6.13 shows the Arrhenius plot, ln k versus the reciprocal absolute temperature (1/T). Slope of the straight line gives an activation energy of 54.5 ± 1 kJ/mol for nickel(0) nanoclusters catalyzed hydrolysis of sodium borohydride.

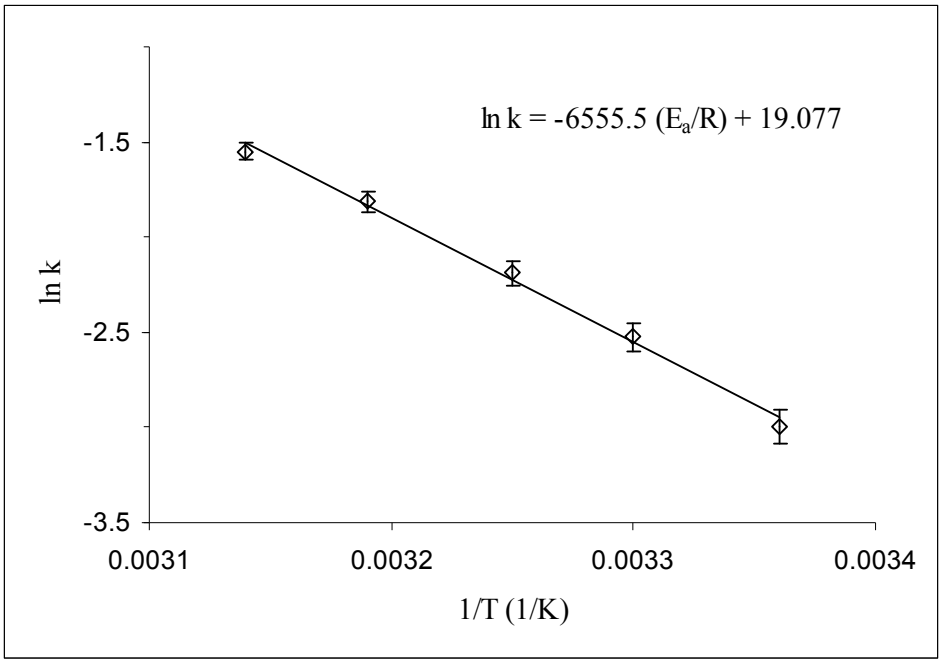

Figure 6.13. The Arrhenius plot, ln*k* versus the reciprocal absolute temperature 1/T, for the hydrolysis of sodium borohydride catalyzed by hydrogenphosphate-stabilized nickel(0) nanoclusters in the temperature range is 25- 45 ^{o}C.

Compared to the activation energies reported for the other catalysts used in the hydrolysis of sodium borohydride, Table 6.2, this is a quite low value, close to the one obtained for the ruthenium(0) nanoclusters catalyzed hydrolysis of sodium borohydride [12].

Table 6.2. Comparison of the activation energies of other catalysts with hydrogenphosphate-stabilized nickel(0) nanoclusters activation energy value for the hydrolysis of sodium borohydride

Catalyst	**Activation Energy ($kJ.mol^{-1}$)**
Nickel (0) nanoclusters	54.5
Ru(0) Nanoclusters	41
Bulk nickel	71
Bulk cobalt	75
$Pt + LiCoO_2$	97

The enthalpy of activation, $\Delta H^{\#}$ and the entropy of activation, $\Delta S^{\#}$ were calculated from the Eyring equation, Eqn **9,** by plotting the graph of $\ln\frac{k}{T}$ versus $\frac{1}{T}$,

$$\ln\frac{k}{T} = \frac{1}{T}\left(\frac{\Delta H^{*}}{R}\right) + \ln\frac{k_b}{h} + \frac{\Delta S^{*}}{R} \qquad \textbf{(9)}$$

Figure 6.14 shows the Erying plot, ln (k/T) versus reciprocal absolute temperature (1/T). The slope of the straight line gives an activation enthalpy of 52.0 ± 1 kJ/mol and the intercept gives activation entropy of -155 ± 3 $J/(mol.K)^{-1}$. The small value of activation enthalpy and the large negative value of activation entropy are indicative of an associative mechanism for the nickel(0) nanocluster-catalyzed hydrolysis of sodium borohydride, consistent with the mechanism suggested for the hydrolysis of sodium borohydride given in the literature [74], involving the formation of BH_5.

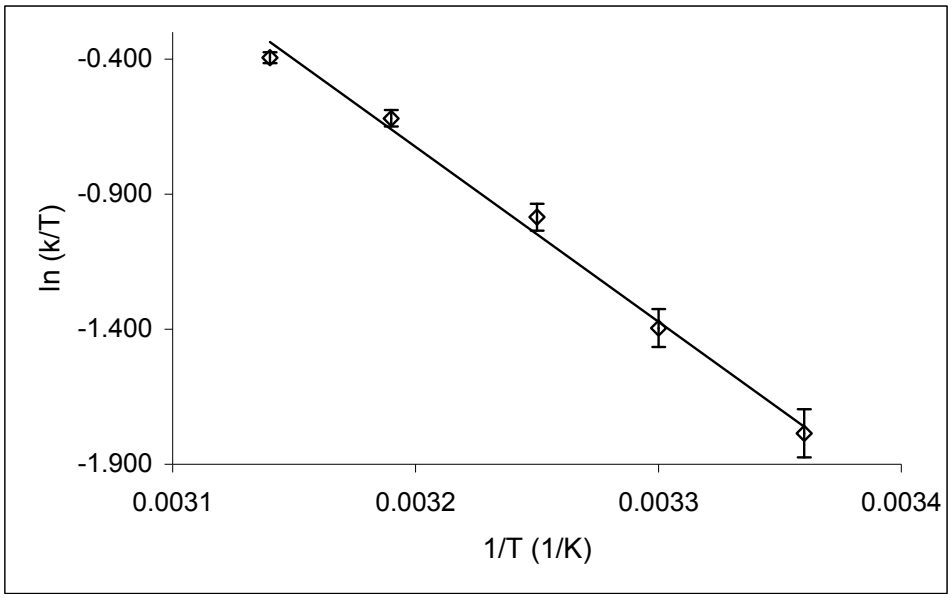

Figure 6.14 The Erying plot, ln (k/T) versus the reciprocal absolute temperature 1/T, for the hydrolysis of sodium borohydride catalyzed by hydrogenphosphate-stabilized nickel(0) nanoclusters in the temperature range 25-45 ^{o}C

CHAPTER 7

CONCLUSIONS

In summary, our study on the synthesis and characterization of hydrogenphosphate-stabilized nickel(0) nanoclusters as catalyst in the hydrolysis of sodium borohydride have led to the following conclusions and insights;

- Nickel(0) nanoclusters can be prepared in-situ during the hydrolysis of sodium borohydride from the reduction of a commercially available precursor material and stabilized by hydrogenphosphate anions in aqueous solution.

- Hydrogenphosphate anion is a good stabilizer for nickel(0) nanoclusters because of excellent size matching between O-O distance (2.52 Å) of hydrogenphosphate and nickel-nickel distance (2.50 Å) on the nanocluster surface.

- Water-dispersible hydrogenphosphate-stabilized nickel(0) nanoclusters are highly active catalysts in the hydrolysis of sodium borohydride even at room temperature.

$$NaBH_4 + 2H_2O \xrightarrow{\text{Ni(0) nanoclusters}} NaBO_2 + 4H_2$$

- Sodium borohydride can be used as hydrogen storage material since it provides a safe and practical mean of producing hydrogen at ambient temperature, when water dispersible hydrogenphosphate-stabilized nickel(0) nanoclusters are used as a catalyst.

- The rate law of the hydrolysis of sodium borohydride catalyzed by the hydrogenphosphate-stabilized nickel(0) nanoclusters can be given as;

$$\frac{-4d[NaBH_4]}{dt} = \frac{d[H_2]}{dt} = k[Ni]$$

The catalytic hydrolysis of sodium borohydride is first order with respect to the catalyst concentration and zero order with respect to the substrate concentration.

- The activation energy (E_α), activation enthalpy ($\Delta H^{\#}$) and activation entropy ($\Delta S^{\#}$) of hydrogenphosphate-stabilized nickel(0) nanoclusters catalyzed hydrolysis of sodium borohydride were found to be 54.5 ± 1 kJ/mol, 52 ± 1 kJ/mol and -155 ± 3 J/K.mol, respectively. These values imply on an associative mechanism for the hydrolysis of sodium borohydride.

- Hydrogenphosphate-stabilized nickel(0) nanoclusters are highly active catalyst with long lifetime providing 1450 total turnovers in the hydrolysis of sodium borohydride over 4 hours before they are deactivated. The recorded turnover frequency (TOF) is 6.04 min^{-1}.

- The results of the poisoning experiment suggest that 11% of total nickel atoms were found to be active in the catalytic hydrolysis of sodium borohydride.

REFERENCES

1. Energy Information Administration, Annual Energy Outlook 2005 With Projections To 2025, www.eia.doe.gov/oiaf/aeo/pdf/0383(2005).pdf, February 2005,

2. U. S. Department of Energy, Basic Research Needs For the Hydrogen Economy, Report of the Basic Energy Sciences Workshop on Hydrogen Production, Storage and Use , www.sc.doe.gov/bes/hydrogen.pdf, May 13-15, 2003

3. (a) Amendola, S.C.; Janjua, J.M.; Spencer, N.C.; Kelly, M.T.; Petillo, P.J.; Sharp-Goldman, S.L.; Binder, M., *Int. J. Hydrogen Energy*, **2000**, 25, 969-975. (b) Lee, J.Y.; Lee, H.H., Lee, J. H., Kim D.M., Kim J.H. *J. Electrochem. Soc*., **2002**, 149(5), A 603-606.

4. Kaufman, C. M., Sen, B., *J. Chem. Soc. Dalton. Trans.*, **1985**, 83, 307-313.

5. Levy, A.; Brown, J. B.; Lyons, C. J.; *Ind. Eng. Chem.*, **1960**, 52, 211-214.

6. Brown, H.C.; Brown C.A., *J. Am. Chem. Soc.,* **1962**, 84, 1493-1494.

7. Korobov II.; Mozgina, N. G.; Blinova, L. N., *Kinet. Catal*., **1995**, 48(3), 380-384.

8. Amendola, S.C.; Onnerud, P.; Kelly, M.T.; Petillo, P.J.; Sharp-Goldman, S.L.; Binder, M., *J.Power Sources,* **2000**, 85, 186-189.

9. Kojima, Y.; Suzuki, K.I.; Fukumoto, K.; Sasaki, M.; Yamamoto, T.; Kawai, Y.; Hayashi, H., *Int. J. Hydrogen Energy*, **2002**, 27, 1029-1034.

10. Hua, D.; Hanxi, Y.; Xinping, A.; Chuansain, C., *Int. J. Hydrogen Energy,* **2003**, 28, 1095.

11. Kim, J.H.; Lee, H.; Han, S.C.; Kim, H.S.; Song, M.S.; Lee, J.Y., *Int. J. Hydrogen Energy*, **2004**, 29, 263-267.

12. Özkar S.; Zahmakıran M., J.Alloys and Comp., **2005,** 404-406, 728-731

13. (a) Aiken J.D.; Finke R.G., Journal of Molecular Catalysis(A:Chemical) **1999**, 145, 1-44. (b) Roucoux A.; Schulz J.; Patin H., Chem Rev. **2002**, 102 , 3757-3778 (c) Widegren J.; Finke R.G., Journal of Molecular

Catalysis (A:Chemical), **2003**, 198, 317-341. (d) Özkar S.; Finke RG., J. Am. Chem. Soc., **2002**, 124, 5796-5810

14. Amendola S.C.; Janjua J.M.; Spencer N.C.; Kelly M.T.; Petillo P.J.; Sharp-Goldman S.L.; Binder M., Int.J.Hydrogen Energy, **2000,** 25, 186

15. Finke R.G.; Özkar S., Coordination Chem. Rev., **2004,** 248, 135-146

16. Özkar S.; Finke R.G., Langmuir, **2003,** 19, 6247-6260

17. Orgul, S., Yıldırım, S., Proceedings International Hydrogen Energy Congress and Exhibition IHEC 2005 Istanbul, Turkey, 13-15 July **2005**

18. European Commission High Level Group on Hydrogen and Fuel Cell Technologies Summary Report, Hydrogen Energy and Fuel Cells, A Vision for Our Future, June **2003**.

19. Sherif S.A.; Barbir F.; Veziroğlu T.N., Solar Energy, **2005,** 78, 647-660

20. Sossina, M.H., *Acta Materialia.,* **2003**, 51, 5981-6000

21. (a) Amendola S.C.; Onnerud, P.; Kelly, M.T.; Petillo, P.J; Sharp, G.L.; Binder, M., *J .Power Source,* **2000**, 85, 186. (b) Amendola S.C.; Janjua, J.M.; Spencer, N.C.; Kelly, M.T.; Petillo, P.J.; Sharp, G.L.; Binder, M., *Int. J. Hydrogen Energy,* **2000**, 25, 969. (c) Lee, J.Y.; Lee, H.H.; Lee, J.H.; Kim, D.M.; Kim, J.H., *J. Electrochem. Soc.,* **2002**, 149 (5), 603.

22. Schlesinger H.I; Brown H.C; Finholt A.B; Gilbreath J.R; Hockstra H.R; Hydo E.K., *J. Am. Chem. Soc*., **1953**, 75**,** 215.

23. (a) Levy A., Brown J.B, Lyons C.J., *Ind. Eng. Chem.*; **1960**, 52, 211. (b) Kaufman C.M, Sen B., *J. Am. Chem. Soc. Dalton Trans.*; **1985**, 307. (c) Brown H.C, Brown C.A., *J. Am. Chem. Soc.*; **1962**, 84, 1493.

24. James B.D, Wallbridge MGH., *Prog. Inorg. Chem*.; **1970,** 11, 99-231.

25. Aicllo R, Sharp J.H, Matthews M.A., *Int. J. Hydrogen Energy*; **1999**, 24**,** 1123-1130.

26. Davis W.D, Mason L.S, Stegaman G., *J. Am. Chem. Soc.*, **1949**, 71, 2775.

27. Aiken III J.D., Lin Y., Finke R.G., J. Mol. Catal. A:, **1996,** 114, 29-51

28. Schmid G. (Ed), Clusters and Colloids: From Theory to Applications, VCH Publishers, New York, **1994**

29. Jongh L.J.(Ed), Physics and Chemistry of Metal Cluster Compounds, Kluwer Publishers, Dordrect, **1994**

30. Simon, U., Schön, G., Schmid, G., *Angew Chem. Int. Ed. Eng*., **1990**, 248, 1186.

31. Glanz, J., *Science*, **1995**, 269, 1363.

32. Antonietti, M.; Göltner, C.; *Angew Chem. Int. Ed. Eng.*, **1997**, 36, 910.

33. Elghanian, R.; Storhoff, J.J.; Mucic, R.C.; Setinger, R.L.; Mirkin, C.A.; *Science*, **1997**, 277, 1078.

34. Colvin, V.L., Schlamp, M.C., Alivisatos, A.P., *Nature*, **1994**, 370, 354.

35. Sonti, S.V., Bose, A., *J. Colloid Int. Sci*., **1995**, 170, 575.

36. Vossmeyer, T., Delenno, E., Heath, J.R., *Angew. Chem., Int. Ed. Eng*., **1997**, 36, 1080.

37. (a)Schmid, G., Maihack, V., Lantermann, F., Pechel, S., *J. Chem. Soc. Dalton Trans.*, **1996**, 199, 589 (b) Lin, Y., Finke, R. G., *J. Am. Chem. Soc.*, **1994**, 116, 8335. (c) Bönneman, H.; Braun, G.A., *Angew Chem. Int. Ed. Eng*., **1996**, 35, 1992. (d) Lewis, L.N.; Lewis, N., *J. Am. Chem. Soc.*, **1986**, 108, 7228. (e) Wilcoxon, J.P.; Martinho, T.; Klavetter, E.; Sylwester, A.P., *Nanophase Mater*. **1994**, 771. (f) Na, Y.; Park, S.; Bong, S.H.; *J. Am. Chem. Soc.*, **2004**, 126, 250. (g) Pelzer, K.; Vidoni, O.; Phillot, K.; Chaudret, B.; Colliére, V., *Adv. Func. Mater*., **2003**, 12, 118. (h) Hostetler, M.; Wingate, J.; Zong, C.; Evans, N.; Murray, R., *Langmuir*, **1998**, 14, 17-30 (ı) Pelzer, K.; Phillot, K.; Chaudret, B., *Z. Anorg. Allg. Chem.*, **2003,** 629, 1217.

38. Pool R., Science, **1990,** 248, 1186-1188

39. Overbeek J.T.G., In Colloidal Dispersions, J.W. Goodwin (ed.), RSC, London, **1981**

40. Faraday M., Phil.Trans.Roy.Soc., **1857**, 147, 145

41. Klabunde K.J. (Ed), Nanoscale Materials in Chemistry, Wıley-Interscience Publishers, Newyork, **2001**

42. Blatchford C. G.,. Campbell J. R, Creighton J. A., Surface Science, **1982**, 120, 435

43. Schmid, G., Pfeil, R., Boese, R., Bandermann, F., Meyers, S., Calis, G.H.M., Van Der Velden, J.W.A. Chem. Ber., **1981**, 114, 3634

44. Amiens, C., De Caro, D., Chausret, B., Bradley, J. S., Mazel, R., Roucau, C.J., J.Am.Chem.Soc., **1993**, 115, 11638

45. Vidoni, O., Philippot, K., Amiens, C., Chaudret, B., Balmes, O., Malm, J. O., Bovin, J. O., Senocq, F., Casanove, M., J.Angew.Chem, Int. Ed., **1999**, 38, 3736

46. Roucoux A., Schulz, J., Patin, H., Chem. Rev., **2002**, 102, 3757-3778

47. Hirai, H., Nakao, Y., Toshima, N., J. Macromol. Sci., Chem. **1978**, *A12*, 1117.

48. Hirai, H., Nakao, Y., Toshima, N., *J.* Macromol. Sci. Chem.*,* **1979**, *A13*, 727.

49. Hirai, H., J. Macromol. Sci. Chem.*,* **1979**, *A13*, 633.

50. Hirai, H., Makromol. Chem. Suppl., **1985**, *14*, 55.

51. Hirai, H., Nakao, Y., Toshima, N., Chem. Lett.*,* **1978**, 545.

52. Tan, C. K.; Newberry, V.; Webb, T. R.; McAuliffe, C. A., *Dalton Trans.* **1987**, 1299.

53. Boutonnet, M.; Kizling, J.; Stenius, P.; Maire, G., *Colloids Surf.,* **1982**, *5*, 209.

54. Boutonnet, M., Kizling, J., Touroude, R., Maire, G., Stenius P., *Appl. Catal.,* **1986**, *20*, 163.

55. Van Rheenen, P.; McKelvy, M.; Marzke, R.; Glaunsinger, W. S., *Inorg. Synth.,* **1983**, *24*, 238.

56. Balogh, L.; Tomalia, D. A., J. Am. Chem. Soc.*,* **1998**, *120*, 7355.

57. Zhao, M.; Sun, L.; Crooks, R. M., J. Am. Chem. Soc.*,* **1998**, *120*, 4877.

58. Zhao, M.; Crooks, R. M., Angew. Chem., Int. Ed. Engl.*,* **1999**, *38*, 364.

59. Nakao, Y.; Kaeriyama, K. J., Colloid Interface Sci.*,* **1986**, *110*, 82.

60. Smith T.W., US Patent 4252674

61. Tano T., Esumi K., Meguro K., J. Colloid Interface Sci., **1989**, 133, 530

62. Esumi K., Tano T., Meguro K., Langmuir, **1989**, 5, 268

63. Takahashi Y., Ito T., Sakai S., Ishii Y., Chem. Commun., 1**970**, 1065

64. Aiken III J. D., Finke R.G., J.Moleculear Catalyst, **1999,** 145, 1- 44

65. http://www.uyseg.org/catalysis/pages/cat_frames.htm, 2006

66. Klabunde, K. J., Stark, J., Koper, C., Park, D., *J. Phys. Chem.,* **1996**, 100, 12142.

67. Watzky M. A., Finke R. G., J. Am. Chem. Soc., **1997**, 119, 10382-10400

68. International XPS Spectral Data Processors, www.xpsdata.com, November, 2005

69. Gleason N. R. and Zaera F., J. Catal., **1997,** 169 365

70. Nanda J., Kuruvilla B.A., Sarma D.D., Phys. Rew. B, **1999**, 59, 11

71. Maxted, E.B., *Adv. Catal*., **1951**, 3, 129.

72. (a) Köhler, J.U.; Bradley, J.S., Langmuir, **1998**, 14, 2730. (b) Mc Vicker, G.B.; Baker, R.T.K.; Garten, R.; Kugler, E.L., J. Catal., **1980**, 65, 207.

73. Levine, I.N., Physical Chemistry 3rd edition ; McGraw-Hill Book Company., **1998**

74. (a) Davis, R.E., Swain, C.G., *J. Am. Chem. Soc.*, **1960**, 82, 5950 (b) Mesmer, R.E., Jolly, W.L., *Inorganic Chemistry*, **1962**, 1, 608. In these studies on the acid catalyzed hydrolysis of sodium borohydride, a mechanism has been suggested involving the formation of BH_5 in the transition state; $BH_4 + H^+ \rightarrow [BH_5]^* \rightarrow BH_3 + H_2$. Two activated complexes have been found to be reasonable, one having an attack on hydrogen, the other on boron of the borohydride ion.

APPENDIX A

The kinetic data of the hydrogenphosphate-stabilized nickel(0) nanoclusters catalyzed hydrolysis of sodium borohydride studied by monitoring the hydrogen evaluation depending on substrate concentration, catalyst concentration, stabilizer concentration and temperature.

Table A.1. Volume of hydrogen generated versus time for hydrogenphosphate-stabilized nickel(0) nanoclusters catalyzed hydrolysis of sodium borohydride in different nickel(II) acetylacetonate concentrations. [$NaBH_4$]=150 mM, 25 ± 0.1 ^oC.

Time(s)	1.0 mM	1.2 mM	1.4 mM	1.6 mM	1.8 mM	2.0 mM
0	0	0	0	0	0	0
300	69.36	78.03	78.03	78.03	95.37	104.04
600	112.71	130.05	130.05	147.39	164.73	182.07
900	143.92	164.73	182.07	208.08	230.62	242.76
1200	175.13	199.41	216.75	260.1	286.11	298.25
1500	201.14	230.62	251.43	305.09	334.66	353.74
1800	225.42	258.36	286.11	346.7	383.21	409.23
2100	249.7	286.1	320.79	388.31	431.76	464.72
2400	273.98	313.84	352	429.92	480.31	516.74
2700	298.26	339.85	383.21	471.53	521.92	561.82
3000	319.07	365.86	414.42	509.67	560.06	606.9
3300	339.88	391.87	445.63	547.81	594.74	651.98
3600	357.22	417.88	476.84	585.95	629.42	
3900	374.56	443.89	508.05	620.63	664.1	
4200	391.9	464.7	539.26	655.31		
4500	409.24	485.51	567			
4800	426.58	506.32	594.74			
5100	443.92	523.66	622.48			
5400	461.26	541	650.22			
5700	478.6	558.34				
6000	495.94	575.68				

Table A.2. Volume of hydrogen generated versus time for hydrogenphosphate-stabilized nickel(0) nanoclusters catalyzed hydrolysis of sodium borohydride in different $NaBH_4$ concentrations.

$[Ni(acac)_2]$=1.4 mM, 25 ± 0.1 ^oC.

Time(s)	150 mM	300 mM	450 mM
0	0	0	0
300	78.03	79.76	81.49
600	130.05	133.51	135.24
900	182.07	187.27	189.01
1200	216.75	221.95	225.42
1500	251.43	256.63	261.83
1800	286.11	291.31	298.24
2100	320.79	325.99	333.02
2400	352	358.93	367.8
2700	383.21	391.87	402.58
3000	414.42	424.81	435.52
3300	445.63	457.75	468.46
3600	476.84	488.96	499.67
3900	508.05	520.17	530.88
4200	539.26	551.38	562.09
4500	567	582.59	593.3
4800	594.74	613.8	624.51
5100	622.48	645.01	655.72
5400	650.22	676.8	686.9

Table A.3. A) The volume of hydrogen(mL) versus time(s) in hydrogenphosphate-stabilized nickel(0) nanoclusters catalyzed hydrolysis of sodium borohydride at constant $Ni(acac)_2$ and $NaBH_4$ concentrations, $[Ni(acac)_2]$ =1.4 mM, $[NaBH_4]$=150 mM, at different temperatures (25-45 ^oC) B) The volume of hydrogen(mL) versus time(s) self hydrolysis of sodium borohydride (150 mM) at different temperatures (25-45 ^oC)

		25 °C			**30 °C**			**35 °C**			**40 °C**			**45 °C**	
Time	A	B	A-B	A	B	A-B	A	B	A-B	A	B	A-B	A	B	A-B
300	78.03	17.34	60.69	112.7	17.34	95.37	156.1	26.01	130.1	242.76	43.35	199.41	282.64	69.36	213.28
600	130.1	31.21	98.84	173.4	34.68	138.7	242.8	52.02	190.7	357.19	78.03	279.16	438.7	112.71	325.99
900	182.1	43.35	138.7	222	48.55	173.4	312.1	78.03	234.1	457.72	112.71	345.01	568.75	156.06	412.69
1200	216.8	52.02	164.7	270.5	62.42	208.1	381.5	100.6	280.9	553.07	138.72	414.35	672	190.74	481.26
1500	248	60.69	187.3	319.1	76.29	242.8	450.8	123.1	327.7	648.42	164.73	483.69			
1800	279.2	69.36	209.8	367.6	90.16	277.5	520.2	140.6	379.7						
2100	310.4	78.03	232.4	416.2	104	312.1	589.6	157.8	431.8						
2400	341.6	84.96	256.6	459.5	117.9	341.6	650.3	171.7	478.6						
2700	367.6	91.89	275.7	502.9	126.6	376.3									
3000	393.6	98.82	294.8	537.5	135.2	402.3									
3300	419.6	105.8	313.9	572.2	143.9	428.3									
3600	445.6	112.7	333	606.9	152.6	454.3									
3900	471.6	119.6	352	641.6	161.3	480.3									
4200	497.7	126.5	371.1	672	169.9	502.1									
4500	518.5	133.5	385												
4800	539.3	138.7	400.6												
5100	560.1	143.9	416.2												
5400	580.9	149.1	431.8												
5700	598.2	154.3	444												
6000	615.6	159.5	456.1												